Global Biogeochemical Cycles

RESEARCH ARTICLE
10.1029/2024GB008250

Key Points:

- We used the dominant source layer framework to evaluate riparian-stream connectivity in four forest headwater catchments across Europe
- Hydroclimate, small-scale topography, and soil characteristics shape differences in riparian hydrology and biogeochemistry across sites
- Riparian-stream relationships can be modulated both by water sources other than the riparian zone and by in-stream biogeochemical processes

Supporting Information:

Supporting Information may be found in the online version of this article.

Correspondence to:

J. L. J. Ledesma,
jose.ledesma@ufz.de

Citation:

Ledesma, J. L. J., Musolff, A., Sponseller, R. A., Lupon, A., Peñarroya, X., Jativa, C., & Bernal, S. (2025). The riparian zone controls headwater hydrology and biogeochemistry, doesn't it? Reassessing linkages across European ecoregions. *Global Biogeochemical Cycles*, *39*, e2024GB008250. https://doi.org/10.1029/2024GB008250

Received 4 JUL 2024
Accepted 21 DEC 2024

Author Contributions:

Conceptualization: José L. J. Ledesma, Andreas Musolff, Susana Bernal
Data curation: José L. J. Ledesma, Andreas Musolff, Anna Lupon, Xavier Peñarroya, Carolina Jativa, Susana Bernal
Formal analysis: José L. J. Ledesma
Funding acquisition: José L. J. Ledesma
Investigation: José L. J. Ledesma, Anna Lupon, Xavier Peñarroya, Carolina Jativa, Susana Bernal
Methodology: José L. J. Ledesma
Project administration: José L. J. Ledesma
Visualization: José L. J. Ledesma

The Riparian Zone Controls Headwater Hydrology and Biogeochemistry, Doesn't It? Reassessing Linkages Across European Ecoregions

José L. J. Ledesma[1], Andreas Musolff[1], Ryan A. Sponseller[2], Anna Lupon[3], Xavier Peñarroya[3], Carolina Jativa[3], and Susana Bernal[3]

[1]Department of Hydrogeology, Helmholtz Centre for Environmental Research–UFZ, Leipzig, Germany, [2]Department of Ecology and Environmental Science, Umeå University, Umeå, Sweden, [3]Integrative Freshwater Ecology Group, Centre for Advanced Studies of Blanes—Spanish National Research Council (CEAB-CSIC), Blanes, Spain

Abstract Riparian zones are known to control the hydrology and biogeochemistry of forest headwater catchments. Some evidence suggests that these riparian-stream connections are shaped by a relatively small volume of soil, or *dominant source layer* (DSL), through which most water and solutes are routed laterally. However, the hydrological and biogeochemical significance of the DSL has not been broadly evaluated. We compiled data from four forest headwaters, each from different European sites (boreal, temperate, subhumid Mediterranean, semiarid Mediterranean) to test whether DSL dimensions and biogeochemical characteristics vary predictably across ecoregions based on differences in hydroclimate, topography, and soil features. Boreal DSLs were shallow and thin, whereas small-scale topographic heterogeneity shaped DSL dimensions at the temperate site. In the Mediterranean sites, DSLs were deeper and thicker, but upper riparian layers that seldomly connected to the streams had a large influence on the overall lateral flux. Contrasting hydroclimates and soils led to high dissolved organic carbon concentrations in riparian solutions in both boreal and Mediterranean sites. By contrast, nitrate concentrations were driven by differences in soil saturation, being orders of magnitude higher in dry Mediterranean than in wet temperate and boreal riparian soils. Notably, stream chemistry did not consistently reflect riparian DSL chemistry across flow conditions and ecoregions. We hypothesize that ecoregion-specific water sources bypassing the riparian zone, as well as ecoregion-specific in-stream biogeochemical processes could explain these discrepancies. Overall, conceptualizing the varied roles of the DSL across diverse systems can aid in both scientific assessments and management of land-water connectivity in river networks.

Plain Language Summary Headwaters make up an immense global network that controls the quantity and quality of water in streams, rivers, and larger water bodies downstream. It is well established that soils next to headwater streams, known as riparian zones, play a major role in determining stream chemistry because water from precipitation generally traverses these areas before entering streams. In this study, we compare the role that riparian zones play in boreal, temperate, and Mediterranean forest headwaters. Hydroclimate, topography, and soil characteristics explain differences among ecoregions in the dimensions of the dominant source layer, a soil layer through which most of the water and solutes are supplied from riparian zones to streams. We also found that, under some circumstances, riparian and stream chemistry differed in terms of organic carbon and inorganic nitrogen concentrations. We hypothesize that both water that bypasses the riparian zone in its way to the stream and transformation processes that occur within the stream can explain these differences and contribute to shape stream chemistry. Understanding riparian-stream linkages across ecoregions is important for managing river networks, which provide essential services for human life such as safe drinking water supply, sustainable agricultural production, a viable industry, recreation, and cultural heritage.

1. Introduction

In natural and semi-natural environments, surface water quantity (i.e., discharge) and quality (i.e., chemistry) are largely determined by inputs of matter from the surrounding catchment. Riparian zones, where direct physical interaction between catchment soils and surface waters takes place, are pivotal in controlling the lateral transfer of water and solutes across the terrestrial-aquatic interface, especially in forest headwaters drained by small streams (Naiman & Décamps, 1997; Swanson et al., 1982). Given that up to 80% of the world's fluvial network length

Writing – original draft: José L. J. Ledesma
Writing – review & editing: José L. J. Ledesma, Andreas Musolff, Ryan A. Sponseller, Anna Lupon, Xavier Peñarroya, Carolina Jativa, Susana Bernal

consists of small streams (Benstead & Leigh, 2012; Wohl, 2017), the influence of riparian zones on worldwide biogeochemical cycling and overall quality of surface waters is disproportionally large.

Understanding the processing and mobilization mechanisms of dissolved organic carbon (DOC) and nitrogen species, particularly the more mobile nitrate ($N–NO_3^-$), has been a major focus of research in riparian studies because these solutes play significant roles in catchment biogeochemical cycling and water quality (e.g., Cirmo & McDonnell, 1997; Tiegs et al., 2019). DOC controls the acidification status of surface waters (Bishop et al., 1990), affects the bioavailability and mobility of metals and organic pollutants (Bergknut et al., 2010; Shafer et al., 1997), and interferes with drinking water production processes downstream (Chow et al., 2003; Lavonen et al., 2013; Raeke et al., 2017). Elevated concentrations of $N–NO_3^-$ in surface waters can lead to acidification and, more commonly, eutrophication and consequent ecosystem impairment (Camargo & Alonso, 2006). Moreover, both DOC and $N–NO_3^-$ play a fundamental role in the ecology and metabolic activity of aquatic biota, which ultimately has important implications for the global carbon and nitrogen cycles via greenhouse gas emissions (Battin et al., 2023; Cole et al., 2007; Soued et al., 2016).

The importance of riparian zones in shaping catchment hydrology and biogeochemistry has been widely established in the literature, including the idea that they are biogeochemical "hot spots" that connect the catchment to the stream during hydrological "hot moments" (McClain et al., 2003; Vidon et al., 2010). More recently, the dominant source layer (DSL) concept was introduced to provide a framework for testable hypotheses on the importance of riparian processes (Ledesma, Futter, et al., 2018). The DSL framework focuses on the often-ignored vertical dimension in hydrological connectivity between riparian zones and streams (Li et al., 2020), and how it juxtaposes with vertical heterogeneity in riparian biogeochemistry. Consequently, the DSL framework explicitly addresses spatial and temporal variability in riparian subsurface water chemistry, which is generally poorly characterized because relevant data are difficult to collect.

The DSL is defined as the riparian zone depth stratum through which most of the water and solutes are supplied to streams and builds upon the transmissivity feedback mechanism and the Riparian Flow-Concentration Integration Model (Rodhe, 1989; Seibert et al., 2009). Typically, lateral water flow exports from riparian zones to streams exponentially increase as the groundwater table rises and water enters upper, highly conductive riparian soil layers during rainfall or snowmelt events. This mechanism is observed via non-linear relationships between the riparian groundwater table and stream discharge (Frei et al., 2010; Kendall et al., 1999). The chemical signature of each riparian soil depth can be assumed to be imprinted in the laterally flowing water traversing it, and this signal is then transferred to the stream, explaining the mirroring between riparian and stream chemistry (Bishop et al., 2004). While examples of riparian-stream hydrological and biogeochemical coupling exist for most ecoregions, including boreal (Ledesma, Futter, et al., 2018), temperate (Musolff et al., 2018), Mediterranean (Bernal et al., 2015), and tropical (McDowell et al., 1992) forests, hydrochemical data establishing the dimension and overall significance of the DSL across systems are lacking. Most riparian studies rely on single catchment approaches or focus on a single ecoregion and thus have only a modest value for universal generalizations of the specific hydrological and biogeochemical processes involved. Furthermore, research on riparian-stream interactions and, by extension, catchment hydrology and biogeochemistry has not been developed to the same extent across ecoregions and is biased towards northern temperate (e.g., Campbell et al., 2021) and boreal (e.g., Laudon et al., 2021) landscapes. At the continental level of Europe, this bias implies a knowledge limitation on the more heterogeneous, and potentially more complex Mediterranean ecoregion (Bernal et al., 2013).

Despite the overall consensus about the importance of riparian zones, it is still debated whether they are the only or even the major driver of stream chemistry in forest headwaters. Water inputs from upslope or from deep groundwater sources that bypass the riparian soils, as well as biogeochemical processes taking place within the aquatic compartment, might collectively weaken or mask the chemical influences of riparian processes on stream chemistry (Hruška et al., 2014; Marcé et al., 2018; Roebuck et al., 2023; Sawicka et al., 2016). Spatial hydrological and biogeochemical heterogeneity in the riparian zone complicates teasing apart the relative importance of the different drivers (Bernhardt et al., 2017; Grabs et al., 2012). Therefore, there is a need to explore the extent to which riparian zones determine stream chemistry in forest headwaters, particularly in relation to major biogeochemical drivers such as DOC and $N–NO_3^-$. The DSL concept assumes that all water entering the stream (a) comes from the riparian zone and (b) does not experience major biogeochemical changes in the aquatic compartment, and thus can be used to precisely test whether these assumptions are satisfied. This ability, combined with the detailed representation of subsurface lateral water and solute fluxes, provides a suitable framework to test whether stream chemistry reflects riparian soil water chemistry. Other frameworks based on the mixing of distinct source waters, including classical endmember mixing analyses or more recent approaches such as the shallow and deep hypothesis (Hooper et al., 1990; Stewart et al., 2022; Zhi & Li, 2020), might not fully capture the complexity of site-specific lateral subsurface fluxes in this context.

Here we provide an empirical synthesis supported by conceptualizations of our fundamental understanding of processes controlling water transfer and solute transformation and mobilization between riparian zones and streams across four European ecoregions. We present data from the boreal *Krycklan*, the temperate *Rappbode*, the subhumid Mediterranean *Font del Regàs*, and the semiarid Mediterranean *Fuirosos* forest headwaters. These sites have been the subjects of much research in the past and are considered representative of their specific ecoregions. We integrate the knowledge and data produced in these previous studies with new data collected for this synthesis. Our main goal was to define common patterns and specific differences in riparian hydrological behavior (including the thickness and vertical position of the DSL) and riparian biogeochemistry (represented by DOC and $N–NO_3^-$ concentrations) across the four sites. Subsequently, we use the DSL framework to explore the extent to which stream DOC and $N–NO_3^-$ reflect riparian soil water DOC and $N–NO_3^-$ in these forest headwater catchments. This exploratory exercise enabled us to hypothesize mechanisms that potentially explain discrepancies in chemistry between riparian zones and streams.

2. Study Sites, Data, and Methods

2.1. Characterization of Study Sites

The Krycklan Catchment Study, located in northern Sweden (Figure 1a; Table 1), has been used since the 1980s for hydrology, biogeochemistry, and climate research in the boreal landscape (Laudon et al., 2021). In this study, we focus on the subcatchment Västrabäcken, known as C2.

The upper Rappbode catchment, located in the Harz mountains of central Germany (Figure 1b; Table 1), has been studied and monitored since the early 2010s for understanding catchment controls on solute exports in temperate sites (e.g., Werner et al., 2021). The catchment experienced a pronounced drought in the years 2018 and 2019, which led to a large infestation of trees by bark beetles (Musolff et al., 2024; Rakovec et al., 2022). This infestation resulted in the removal of most of the upslope Norway spruce forest in the years 2020 and 2021 (Kong et al., 2022).

The Font del Regàs catchment, located in the Montseny Natural Park in northeastern Spain (Figure 1c; Table 1), was initially studied in the early 2010s and more regularly monitored since 2018 for understanding catchment hydrology and biogeochemistry of Mediterranean systems (Ledesma, Lupon, & Bernal, 2021; Lupon, Bernal, et al., 2016).

The Fuirosos catchment, located in the Montnegre-Corredor Natural Park, also in northeastern Spain (Figure 1d; Table 1), has been studied since the late 1990s at irregular intervals with a strong focus on understanding riparian hydrology and biogeochemistry of intermittent systems (Bernal et al., 2005; Butturini, 2021; Ledesma, Lupon, & Bernal, 2021). Contrary to the other three streams, which are all perennial, the Fuirosos stream is intermittent and ceases flowing during the driest months of the year, typically from late June to late September.

2.2. Data Availability

2.2.1. Meteorological Data, Stream Discharge, and Stream Chemistry

Mean temperature and precipitation data were available for all sites at different periods and from different sources (Table 1). At Krycklan, daily values (1981–2022) come from a meteorological station located a few hundred meters from the outlet of the C2 catchment. At Rappbode, long-term mean annual temperature was reported by Werner et al. (2019) and mean annual precipitation (1986–2015) was available from Musolff et al. (2021). At Font del Regàs and Fuirosos, daily values (2009–2022) were available from two meteorological stations managed by the Catalan Meteorological Service. Viladrau station is located ca. 4 km northwest of the outlet of Font del Regàs, whereas Dosrius is located ca. 15 km southwest of the outlet of Fuirosos. The representativeness of the meteorological data from these two stations was previously assessed and considered descriptive for both catchments (Ledesma, Lupon, & Bernal, 2021).

10.1029/2024GB008250

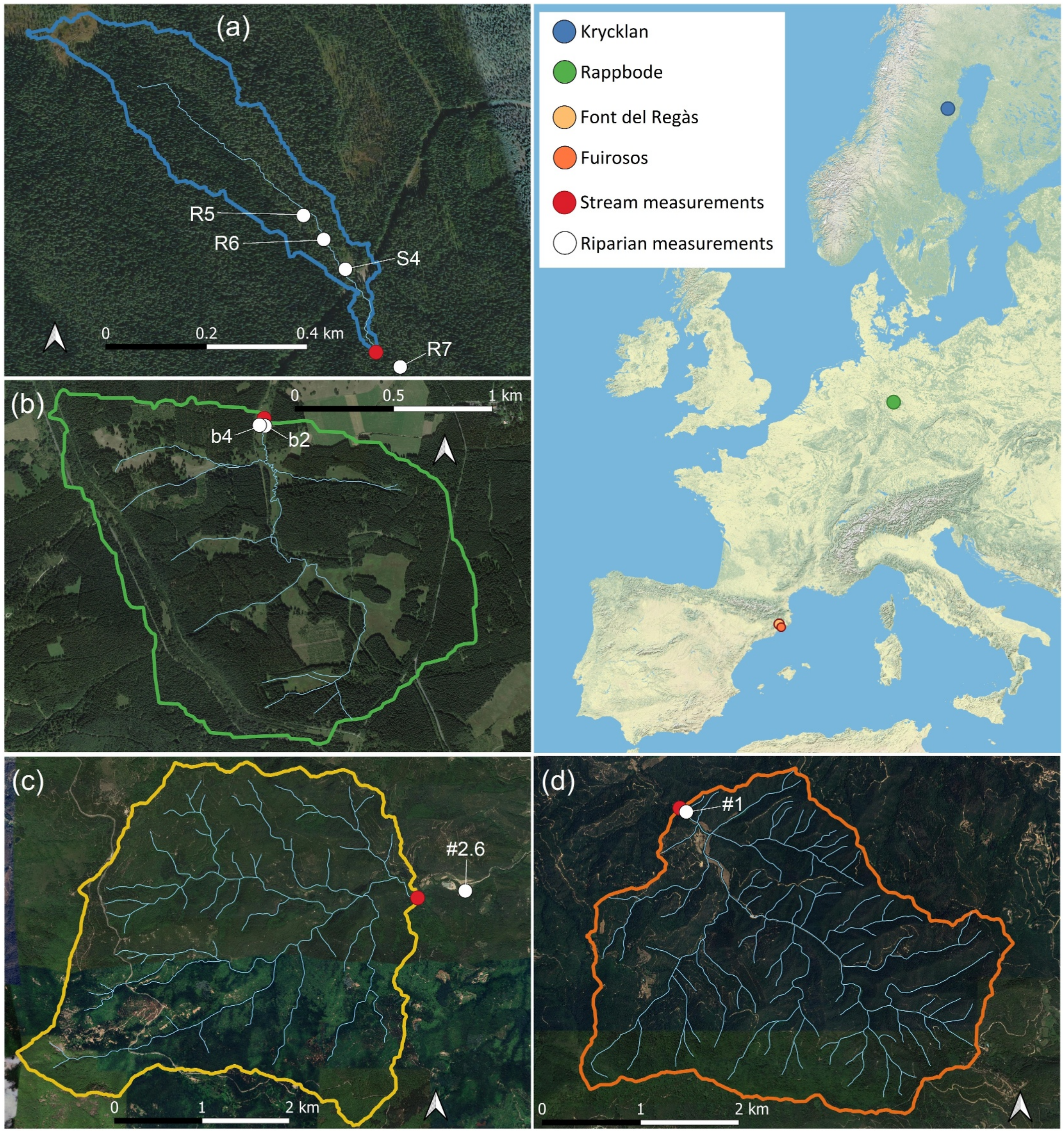

Figure 1. Location of study sites within Europe and catchment delineations at the location where we measured stream discharge for (a) the boreal *Krycklan* C2, (b) the temperate upper *Rappbode*, (c) the subhumid Mediterranean *Font del Regàs*, and (d) the semiarid Mediterranean *Fuirosos*. Background maps: ESRI Physical and Google Satellite in QGIS 3.30.

Stream discharge data were available for different drainage areas at daily frequencies from all sites, except for a few missing days due to device failure (Table 1; Table 2). Stream DOC and N–NO_3^- concentrations were available at various intervals, but most commonly biweekly at all sites (Table 2). No stream chemistry was available from Fuirosos for a 3-month period when the stream ceased flowing (July–September 2022). The available data periods varied across sites and between DOC and N–NO_3^- (Table 2).

2.2.2. Riparian Groundwater Tables and Soil Water Chemistry

As part of the Riparian Observatory in Krycklan (Grabs et al., 2012), three riparian soil profiles were established in 2007 representing the riparian zones in the C2 catchment (R5, R6, and R7). Each profile was 2–4 m from the stream and consisted of two ceramic suction cups at each of five equally distributed soil depths for soil water collection (Table 2). Soil water DOC concentrations were available from eight sampling campaigns (June 2008 to September 2009) and, only for profile R5, from seven additional campaigns (June 2013 to May 2014).

Table 1
Characteristics of the Study Sites

	Krycklan C2	Upper Rappbode	Font del Regàs	Fuirosos
Ecoregion	Boreal	Temperate	Subhumid Mediterranean	Semiarid Mediterranean
Mean annual temperature (°C)	2.1 (1981–2022)	6.0 (long-term)[a]	11.3 (2009–2022)	14.1 (2009–2022)
Mean annual precipitation (mm)	638 (1981–2022)	1061 (1986–2015)[b]	964 (2009–2022)	663 (2009–2022)
Snow	ca. 30% of precipitation[c]	Accumulates in winter	<1%[d]	Virtually non-existent
Mean annual PET[e] (mm)	526 (1985–2019)[f]	665 (1986–2015)	989 (2004–2006)[g]	1393 (2004–2006)[g]
Dryness index[h]	0.83	0.63	1.03	2.10
Evaporative index[i]	0.64 (2009–2017)	0.53 (2013–2022)	0.74 (2020–2022)	0.91 (2019–2022)
Discharge measurement location	64° 15’ N, 19° 46’ E	51° 39’ N, 10° 42’ E	41° 49’ N, 2° 27’ E	41° 43' N, 2° 34' E
Discharge point drainage area (km^2)	0.12	2.58	13.0	9.94
Elevation range (m a.s.l.)	243–306	540–620	503–1603	169–758
Upslope vegetation	Pine and spruce forest	Pine and spruce forest	Beech and oak forest	Pine and oak forest
Riparian vegetation	Spruce and birch forest	Grasses	Mixed deciduous forest	Mixed deciduous forest
Riparian width (m)	5–40	40 (at lower part)	10–20 (at lower part)	10–20 (at lower part)

[a]Werner et al. (2019). [b]Musolff et al. (2021). [c]Laudon et al. (2021). [d]Lupon, Bernal, et al. (2016). [e]Potential evapotranspiration estimated with the Penman–Monteith equation. [f]Gutierrez Lopez et al. (2021). [g]Bernal et al. (2012). [h]Ratio of PET to precipitation. [i]Ratio of actual evapotranspiration to precipitation.

Representative solute concentrations for each depth were estimated as the average of the two values coming from the pair of suction cups. No N–NO_3^- concentrations were available for these profiles.

Further, a hillslope transect was installed close to the outlet of catchment C2 in autumn 1995. This transect consists of three soil profiles located at 4, 12, and 22 m from the stream following the local topographic slope. The riparian profile (S4) included ceramic suction cups placed at six depths (Table 2). At S4, soil water DOC concentrations were available for 56 sampling campaigns for the most superficial suction cup and for 122 to 134 campaigns for the other suction cups (1996–2022). Soil water N–NO_3^- concentrations were available for three sampling campaigns for the most superficial suction cup and for 23 to 38 campaigns for the other suction cups (2013–2022).

A perforated monitoring well equipped with a TruTrack water level data logger was installed alongside the four riparian profiles at C2 to record groundwater tables. Daily groundwater table records were available for profiles R5, R6, and R7 (May 2008 to September 2009) and for profile S4 (June 2013 to September 2014) (Table 2). The four profiles are representative of the catchment because they are located in areas of high topographic wetness index (TWI), which contribute the most to water and solute fluxes to the stream (Grabs et al., 2012; Leach et al., 2017).

In September 2021, two riparian profiles were established at Rappbode near the catchment outlet in a well-studied 50 m × 50 m riparian plot, characterized by relatively flat terrain and a higher TWI compared to the rest of the catchment (Werner et al., 2021). One riparian profile was located 10 m from the stream at a location with relatively low TWI, representing dry riparian areas in which the groundwater table varies along a large depth range. The second profile was located 15 m from the other side of the stream at a location with relatively high TWI, representing wet riparian areas in which the groundwater table is often close to the surface. The dry and wet areas in the riparian zone at Rappbode have distinct hydrological and biogeochemical behaviors and contribute an estimated ca. 60% and 40% of water fluxes to the stream, respectively (Werner et al., 2021).

Ceramic suction cups were installed at three depths at the profile with low TWI, and at two depths at the profile with high TWI (Table 2). Soil water DOC and N–NO_3N–NO_3^- concentrations were available for eight sampling campaigns (November 2021 to October 2023). The two profiles were located close to existing perforated monitoring wells equipped with pressure transducers (Solinst Levelogger, Canada, and van Essen Micro-Diver, Netherlands) that recorded groundwater tables. Daily groundwater tables were available for wells b2 (next to the “dry” profile) and b4 (next to the “wet” profile) for the period November 2020 to September 2022 (Table 2).

Table 2
Data Availability at the Study Sites

Data	Description	Krycklan (C2)	Upper Rappbode	Font del Regàs	Fuirosos
Stream discharge	Frequency	Daily	Daily	Daily	Daily
	Period	April 2005-September 2022	May 2013–August 2023	January 2020–February 2023	October 2018–February 2023
	Missing data	11%	8%	12%	24%
Stream DOC[a]	Frequency	ca. Biweekly	ca. Biweekly	ca. Biweekly	ca. Biweekly
	Period	July 1987–November 2022	March 2013–November 2014, February 2017–November 2019, October2020–October 2023	November 2021–February 2023	November 2021–February 2023
	N	960	161	31	27
Stream $N–NO_3^-$[b]	Frequency	ca. Biweekly	ca. Biweekly	ca. Biweekly	ca. Biweekly
	Period	July 2008–November 2022	March 2013–November 2014, October 2020–October 2023	November 2021–February 2023	November 2021–February 2023
	N	369	100	32	28
Riparian groundwater table	Profiles	R5, R6, R7, S4	b2 (dry), b4 (wet)	#2.6	#1
	Frequency	Daily	Daily	Daily	Daily
	Period	May 2008–September 2009 (R5, R6, R7) June 2013–September 2014 (S4)	November 2020–September 2022	September 2018–February 2023	October 2019–February 2023
	Missing data	0% (R5, R6, R7), 27% (S4)	24%	10%	26%
Riparian soil water DOC[a]	Depths (cm b.s.s.)[c]	15, 30, 45, 60, 75 (R5, R6, R7) 10, 25, 35, 45, 55, 65 (S4)	10, 30 (b2) 10, 30, 60 (b4)	15, 30, 45, 60, 75, 90, 115	15, 30, 45, 60, 75, 90
	Period	June 2008–May 2014 (R5) June 2008–September 2009 (R6, R7) June 1996–November 2022 (S4)	November 2021–October 2023	May 2021–March 2022	May 2021–March 2022
	N	15 (R5), 8 (R6, R7), 56–134 (S4)	8	3	3
Riparian soil water $N–NO_3^-$[b]	Depths (cm b.s.s.)[c]	10, 25, 35, 45, 55, 65 (S4)	10, 30 (b2) 10, 30, 60 (b4)	15, 30, 45, 60, 75, 90, 115	15, 30, 45, 60, 75, 90
	Period	February 2013-November 2022 (S4)	November 2021–October 2023	May 2021–March 2022	May 2021–March 2022
	N	3–38 (S4)	8	3	3

[a]Dissolved organic carbon. [b]Nitrate. [c]Centimeters below the soil surface.

In May 2021, ceramic suction cups were installed at six depths (Table 2) in a representative riparian profile located 3 m from the Font del Regàs stream at a location where the drainage area is 14.2 km^2, a few hundred meters downstream of the stream discharge measurement location. At that time, we installed an analogous array of suction cups in a representative riparian profile located ca. 7 m from the Fuirosos stream and ca. 70 m upstream the location where stream discharge is regularly monitored (Table 2).

At both Mediterranean sites, soil water was sampled on three occasions for DOC and $N–NO_3^-$ concentrations (May 2021 to March 2022). At Font del Regàs, soil water was additionally sampled at the same times from a piezometer perforated on the bottom 10 cm to a depth of ca. 120 cm. This piezometer was located ca. 30 m downstream of the array of suction cups, also ca. 3 m from the stream, and near a perforated monitoring well. This well (#2.6) was equipped with a HOBO water level data logger that recorded groundwater tables 2 m from the stream. At Fuirosos, a perforated monitoring well (#1), also equipped with a HOBO water level data logger, recorded groundwater tables at the edge of the opposite side of the stream in relation to the array of suction cups. Daily groundwater tables from well #2.6 (September 2018 to February 2023, subhumid Font del Regàs) and well #1 (October 2019 to February 2023, semiarid Fuirosos) were available (Table 2). These two groundwater table time series were considered representative of the corresponding profiles where we measured soil water chemistry after offsetting them using the difference in water level between the wells and suction cup locations (Text S1 in Supporting Information S1). At both sites, the riparian areas where soil water chemistry and groundwater tables were recorded represent the typical riparian groundwater table dynamics, vegetation, and riparian soil characteristics of their corresponding catchments and are hotspots for water accumulation and export to the streams due to their relatively high TWI (Ledesma, Lupon, & Bernal, 2021).

2.3. Using the Dominant Source Layer (DSL) Framework to Study Riparian Zones

The DSL provides an estimation of the riparian zone depth stratum that contributes the most to water and solute fluxes to streams. To assess riparian hydrological behavior across the four study sites, we first established the empirical relationship between the riparian groundwater table and stream discharge, which is the basis of the DSL (Figure S1 in Supporting Information S1). Subsequently, we estimated the thickness and position of the DSL_{90}, that is, the depth range contributing 90% of the total lateral water flux from each riparian profile to the stream (Figure S1 in Supporting Information S1). Additionally, we tested whether stream chemistry matched the expected chemistry from DSL riparian lateral fluxes by comparing flow weighted DOC and $N–NO_3^-$ concentrations in the riparian zone with DOC and $N–NO_3^-$ concentrations in the adjacent stream.

2.3.1. Riparian Groundwater–Stream Discharge Relationships

For each riparian profile, we fitted logarithmic models between matching observations of daily groundwater tables (Gw) and daily stream discharge (Q) so that $Gw = a + k * ln(Q)$. In each case, discharge records were binned at 0.5 cm groundwater table intervals by obtaining the average value within each interval. The binning procedure follows the same approach as Ledesma, Ruiz-Pérez, et al. (2021) and its purpose is twofold: (a) to enhance data consistency by minimizing scattering and (b) to appropriately weight the influence of both low and high stream discharge values given that low flow conditions are predominant, especially at the Mediterranean sites.

In all cases, we applied both a single-logarithmic model and two-logarithmic models (one at each side of a stream discharge tipping point based on a two-step segmented linear regression). The objective of this exercise was to determine the best model fit in each case, choosing between a single- or two-logarithmic models. The criteria for selection included maximizing R^2 (especially at the upper range of the stream discharge), as well as minimizing the difference between the observed and calculated groundwater table at maximum discharge (Table S1 in Supporting Information S1). We prioritized having better estimates at higher discharge values because these conditions are associated with larger lateral fluxes. The process resulted in the selection of a single-logarithmic model for the boreal profiles, and two-logarithmic models for the temperate and Mediterranean profiles (Table S1 in Supporting Information S1).

In our comparison across sites, we considered the coefficient k (cm mm^{-1}) as a proxy for the rate at which upper riparian layers are hydrologically activated in relation to increments in stream discharge. This coefficient represents the vertical stretch (or compression) of the logarithmic function, so that low k values indicate that small increases in groundwater table mobilize large amounts of water (an indication of high hydraulic conductivity), and vice versa (Figure S1 in Supporting Information S1).

2.3.2. Estimation of DSL_{90}

At each riparian profile, we computed riparian lateral water fluxes considering all the dates with observed stream discharge data at each site. First, we used the logarithmic regression equations relating the groundwater table and stream discharge to back-calculate groundwater tables relative to each stream discharge observation to maximize the time series length. Theoretically, for any given stream discharge, lateral fluxes at any given soil depth are proportional to the groundwater table–stream discharge curve (see e.g., Ledesma et al., 2015 for details on the calculations). Two interdependent principles were applied: (a) Darcy's law of proportionality between flow rate and hydraulic gradient and (b) lateral flow only occurring on saturated layers below the groundwater table (Seibert et al., 2009). Each riparian profile was set to be 200 cm deep below the soil surface (b.s.s.) and 50 cm high above the soil surface, which more than covered the range of calculated groundwater table variation across all profiles, and accounted for potential lateral flow overland. The DSL can be specified by estimating the relative contribution of each soil depth (at a 1 cm level of resolution) to the total lateral water flux from the entire profile for any given period of time. Following Ledesma, Ruiz-Pérez, et al. (2021), we quantitatively estimated the DSL_{90}, that is, the depth range contributing 90% of the total lateral water flux (Figure S1 in Supporting Information S1), and compared its extent (i.e., thickness) and vertical position among the different riparian profiles.

2.3.3. Estimation of Riparian Flow-Weighted Concentrations and Riparian–Stream Comparisons

We estimated flow-weighted concentrations of DOC and N–NO_3^- at the different riparian profiles. To do so and considering the whole range of available concentrations, we first constructed three different concentration profiles along the considered depth range (i.e., 50 cm above the soil surface to 200 cm b.s.s.): (a) median, (b) upper quartile (i.e., 75th percentile), and (c) lower quartile (i.e., 25th percentile) DOC and N–NO_3^- concentration profiles. In the three cases (and for both DOC and N–NO_3^-), concentrations were linearly interpolated at a 1 cm resolution across the range of available measurements from the shallowest to the deepest depth where suction cups were placed.

We assumed that the concentration at 200 cm b.s.s. for the boreal and temperate profiles was equal to the lowest concentration measured at the deepest suction cup, and applied linear interpolation from that bottom suction depth to 200 cm b.s.s. Regardless, soil layers below the deepest suction cup had a negligible influence in the calculations for the boreal and temperate profiles. To establish the concentrations at 200 cm b.s.s. at the Mediterranean profiles, we used data collected from deep groundwater stations. At the subhumid site, we used water samples ($N = 27$) from a ca. 3-m-deep piezometer located 10 m from the stream in the studied riparian area. At the semiarid site, we used water samples ($N = 24$) from a ca. 5-m-deep well near the valley bottom. These samples were collected between November 2021 and February 2023. We assumed that the concentration at 200 cm b.s.s. for the three constructed profiles was equal to the median, upper, or lower quartile concentrations, respectively, measured in the samples from the piezometer (subhumid site) and the deep well (semiarid site).

In all cases, concentrations between the shallowest suction cup and the riparian soil surface were assumed to be constant and equal to the concentration at the shallowest suction cup. At 10 cm above the soil surface, we assumed that the DOC concentration was equal to the European average concentration in rain water (Iavorivska et al., 2016), and that the N–NO_3^- concentration was equal to the concentration in wet deposition for the year 2020 for each of the four sites (EMEP, 2023). We linearly interpolated the concentrations between the riparian soil surface (equal to the concentration at the shallowest suction cup) and 10 cm above the surface and assumed a constant concentration between 10 and 50 cm high. This is based on studies that have found concentrations of DOC and N–NO_3^- in water layers of a few centimeters forming above riparian soils to be similar to those in shallow soil layers rather than to atmospheric inputs (Blaurock et al., 2022). Only the wet riparian profile at the temperate site and the riparian profile at the semiarid Mediterranean site showed calculated groundwater tables up to around 10 cm above the soil surface during specific days.

Constructed concentration profiles were then multiplied by the corresponding lateral water flux at each depth and integrated across space in the vertical profile and across time for the available periods (Figure S1 in Supporting Information S1). This integration resulted in a total mass of DOC or N–NO_3^- exported laterally, which divided by the total volume of water laterally exported produces the flow-weighted concentration, which is analogous to a discharge-weighted flux calculated for a given period (Figure S1 in Supporting Information S1). The resulting range in DOC and N–NO_3^- flow-weighted concentrations given by median, upper quartile, and lower quartile concentration profiles were grouped by stream discharge quartiles defined by the availability of stream discharge data.

At each site, we tested whether different flow conditions led to differences in stream DOC and N–NO_3^- concentrations by comparing the four discharge quartile groups using the Kruskal-Wallis test followed by a Dunn's post hoc test for pair comparisons. For each discharge quartile, we then plotted the median of stream DOC and N–NO_3^- concentrations against the median of DOC and N–NO_3^- flow-weighted concentrations from the corresponding riparian zone profiles. The interquartiles from both stream concentrations and riparian flow-weighted concentrations were used as a range estimate to avoid the more extreme values, as our focus was on long-term patterns characterized by moderate situations. In these plots, we interpreted data points within ±20% of the 1:1 line as indicative of stream chemistry being determined mostly by riparian chemistry. We interpreted departures beyond the conservative ±20% uncertainty bounds of the 1:1 line as indicative of either additional water sources bypassing the riparian zone or in-stream biogeochemical processing having an influence on the chemical signal reflected in the stream.

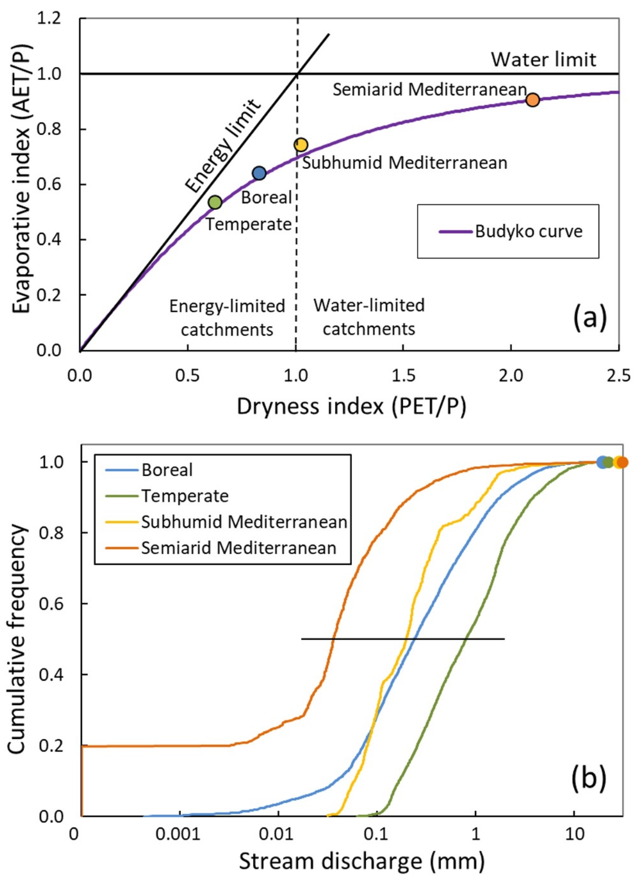

Figure 2. (a) Distribution of the study sites (the boreal *Krycklan* C2, the temperate upper *Rappbode*, the subhumid Mediterranean *Font del Regàs*, and the semiarid Mediterranean *Fuirosos*) in a Budyko plot including the original Budyko hypothesis. (b) Cumulative frequency of stream discharge records for the four sites (the black horizontal line crosses across the median values and the highest values are indicated with a dot).

3. Results and Discussion

3.1. Hydroclimatic Contexts

Our four study sites cover a wide range of hydroclimatic conditions associated with the ecoregions that they represent (Figure 2). All sites fit well in the original Budyko hypothetical curve (Figure 2a) relating dryness index and evaporative index (Budyko, 1974). The semiarid Mediterranean site is the most differentiated of all sites: it is the driest and has the lowest water yield, showing clear evidence of evapotranspiration limitation by water availability (Figure 2a). By contrast, the temperate site is the most humid and has the highest water yield. Here, water availability is high and actual and potential evapotranspiration converge as expected in a typical energy-limited system. The boreal site falls into this characterization as well, but is not as humid due to lower precipitation. The subhumid Mediterranean site is only moderately drier than the boreal site, falling along the boundary between energy- and water-limited systems.

The described climates translate into four significantly different stream discharge distributions (Kruskal-Wallis test, $p < 0.0001$; Figure 2b). The temperate site showed the highest median daily discharge at 0.79 mm, followed by the 0.24 mm median at the boreal site, the 0.20 mm median at the subhumid Mediterranean site, and the 0.04 mm median at the semiarid Mediterranean site (Figure 2b). However, the Mediterranean sites can experience very high daily discharge, including days with higher discharge than the temperate and boreal sites, owing to the occurrence of more severe thunderstorms in this area of Europe (Marchi et al., 2010; Rädler et al., 2019). The semiarid site can also experience days with very low or no discharge; for example, water did not flow during 20% of the days presented here. Mediterranean systems are therefore characterized by more hydrological extremes than boreal and temperate systems (Bernal et al., 2013).

3.2. Riparian Zone Hydrological Behavior

All riparian profiles showed strong non-linear (i.e., logarithmic) relationships between the riparian groundwater table and stream discharge (Figure 3), generally consistent with the transmissivity feedback mechanism (Rodhe, 1989). Nevertheless, the coefficient k of the logarithmic models showcased differences in the riparian zone hydrological behavior among sites. The lowest values of k were observed at the riparian profiles of the boreal site (ranging between 3.0 and 4.5 cm mm^{-1}), indicating that, for each increment in stream discharge, there is a thin riparian layer that is hydrologically activated (Figures 3a–3d; Table S1 in Supporting Information S1). In other words, the activation of the upper riparian layers can mobilize large amounts of water owing to their high hydraulic conductivities. This observation is typical of boreal till riparian soils where shallow layers are highly organic with low bulk density and large structural pores (Ledesma et al., 2015; Nyberg, 1995).

Two-logarithmic models more accurately represented the relationship between the riparian groundwater table and stream discharge in the temperate and Mediterranean profiles (Figures 3e–3h; Table S1 in Supporting Information S1). The thicker or more heterogeneous depth range in which water levels varied here compared to the boreal sites likely explains the more complex fits required. At the temperate dry and wet profiles (Figures 3e and 3f), low discharge was associated with a wide range of possible groundwater tables, owing to the low hydraulic conductivity of these riparian layers (indicated by large k values of 38 and 22 cm mm^{-1}, respectively). At higher discharge values, a vertical compression in the relationships was captured by different logarithmic models with lower k coefficients (i.e., 6.7 and 4.0 cm mm^{-1}, respectively). This observation indicates that shallower riparian layers are more conductive than deeper ones. In agreement, at this and other temperate riparian zones, there is an evident transition from lower mineral, unsorted till layers with lower hydraulic conductivities into upper conductive organic layers, which are nonetheless thinner and contain smaller macropores than at boreal sites (Kendall et al., 1999; Werner et al., 2019).

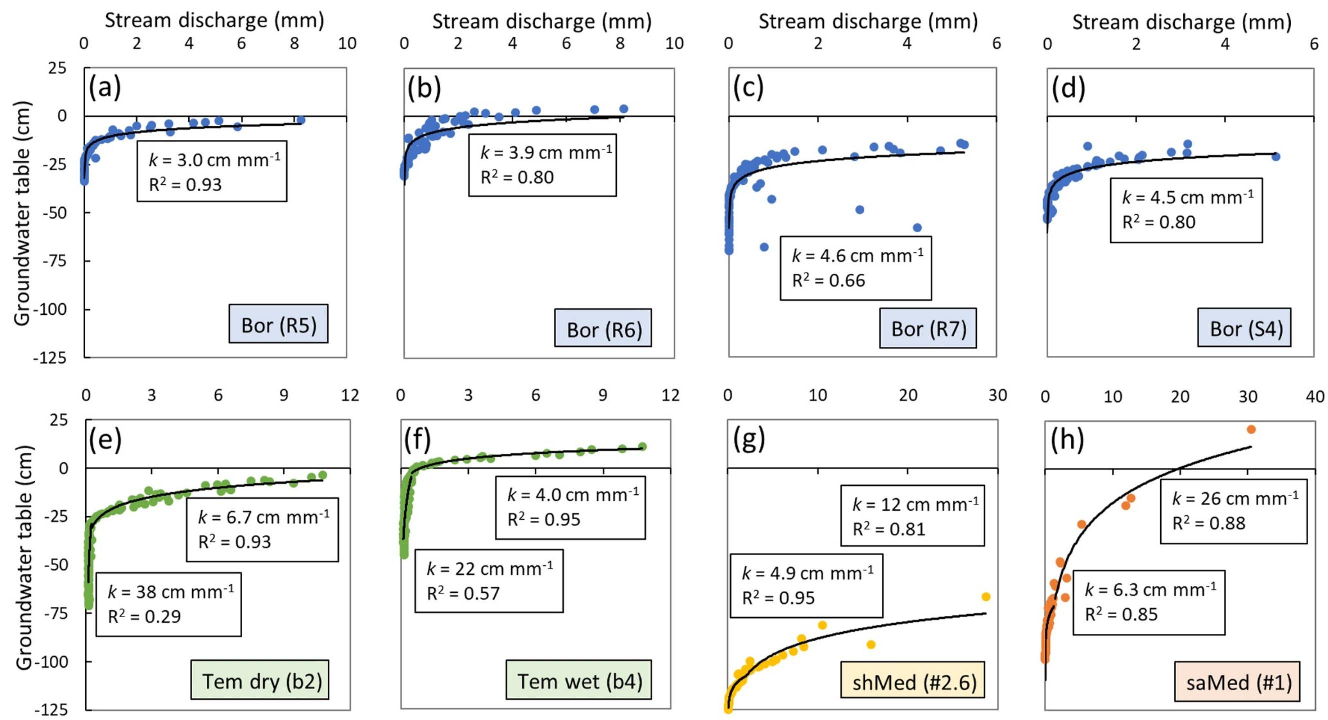

Figure 3. Logarithmic relationships between daily groundwater tables at different riparian profiles and daily discharge at the corresponding streams ($Gw = a + k * ln(Q)$) across four catchments located in (a–d) boreal (Bor), (e–f) temperate (Tem), (g) subhumid Mediterranean (shMed), and (h) semiarid Mediterranean (saMed) ecoregions. Daily stream discharge records were binned at 0.5 cm groundwater table intervals along the riparian profile in order to construct the logarithmic models ($p < 0.0001$ in all cases). Note that the scales of the x-axis differ across panels. Note that in the profiles at the temperate and Mediterranean sites, we fitted two different logarithmic models, one at each side of a tipping point defined by a two-step segmented linear regression model.

The riparian profiles at the subhumid and semiarid Mediterranean sites (Figures 3g and 3h) showed higher k coefficients for periods of high discharge (13 and 26 cm mm^{-1}, respectively) than for periods of lower discharge (5.0 and 6.3 cm mm^{-1}, respectively). However, the tipping points at which the logarithmic relationship shifted corresponded with the 97.5th (2.16 mm) and 98.9th (1.49 mm) percentiles of stream discharge for the subhumid and semiarid sites, respectively (Table S1 in Supporting Information S1). By comparison, the analogous tipping points for the temperate dry and wet profiles corresponded to the 40th and 51st percentiles, respectively. Thus, the unusually high k coefficients observed for the Mediterranean sites at upper riparian layers only apply during exceptionally high flow conditions. We hypothesize that, under those circumstances, a lower effective hydraulic conductivity of shallower layers is induced by pre-existing dry conditions that make exceptionally high precipitation inputs more efficient at filling up the profile vertically relative to the otherwise dominant lateral transmissivity dimension (Fovet et al., 2015; Frei et al., 2012; Ledesma et al., 2022; Tunaley et al., 2016). This behavior appears to be characteristic of Mediterranean sites, especially those of a semiarid context, and not of the boreal and temperate sites. During all other conditions that applied most of the time, riparian groundwater tables in the Mediterranean sites fluctuated through mineral layers. These strata are characterized by sandy or sandy-gravel texture with relatively high hydraulic conductivity (Butturini et al., 2003), which would explain the relatively low k coefficient values during lower discharge.

The vertical distribution of the DSL_{90} was consistent with the differences described based on the k coefficients (Figure 4). At the boreal site, the DSL_{90} was similar across the four available riparian profiles and generally thinner (average thickness = 20 cm) and shallower (average of median depth = 19 cm b.s.s.) than at the other sites (Figures 4a–4d), except for the wet temperate profile. At the temperate site, the DSL_{90} was 30 cm thick for the dry profile (Figure 4e) and 20 cm thick for the wet profile (Figure 4f). The high TWI of the wet profile led to a median DSL_{90} depth of 2 cm above the soil surface, indicating that overland flow was common for the riparian areas represented by this type of profile. By contrast, the low TWI at the dry profile set the median DSL_{90} at 21 cm b.s.s. with no overland flow. We suggest that the small-scale heterogeneous topography (e.g., hollows and hummocks) described for this temperate riparian zone resulted in the divergent position of the DSL_{90} between the wet and dry

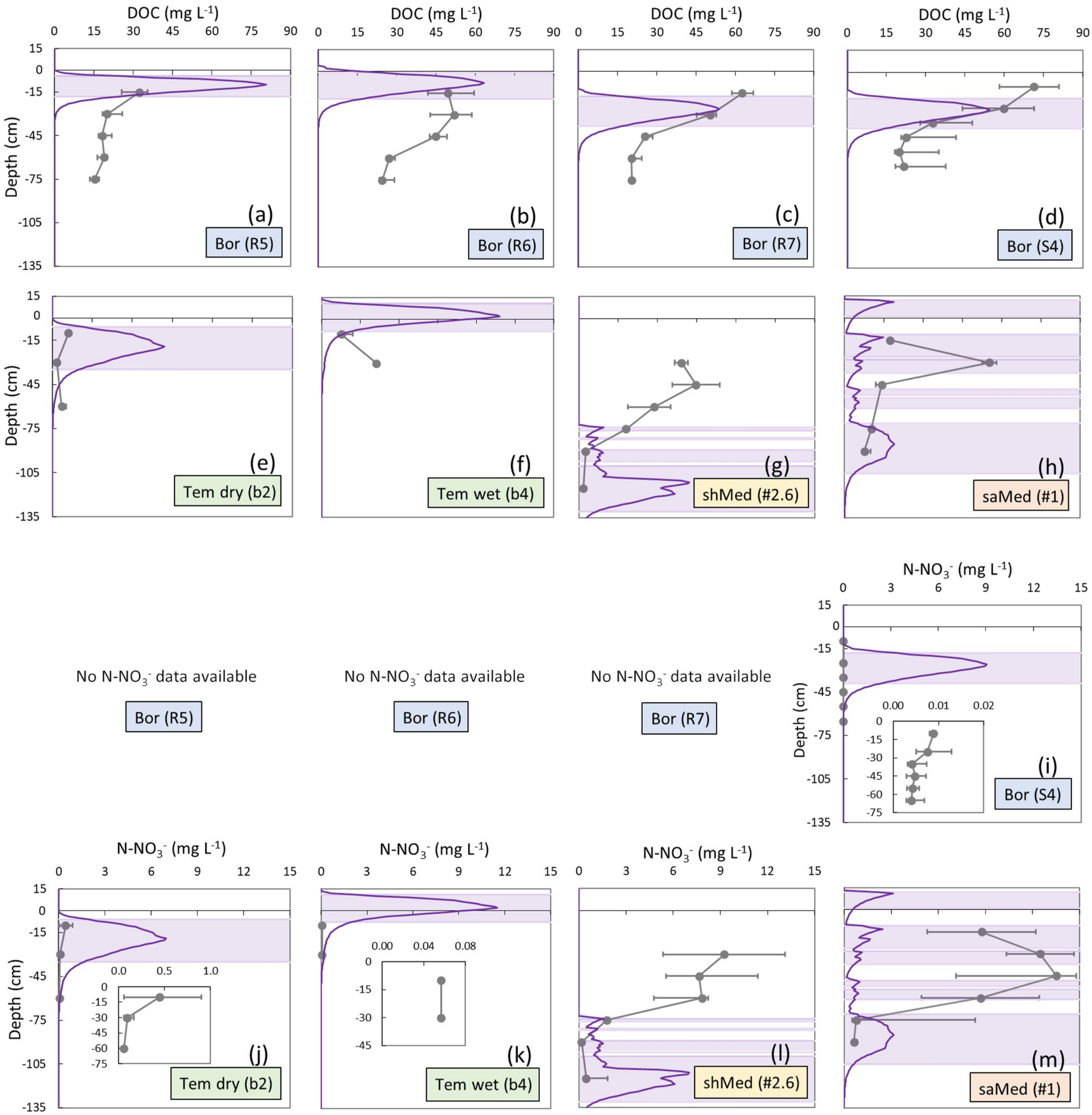

Figure 4. Dissolved organic carbon (DOC) and nitrate ($N–NO_3^-$) concentrations including median (circle) and interquartile range (error bars) at each corresponding depth measured in riparian profiles across four catchments located in (a–d, i) boreal (Bor), (e, f, j, k) temperate (Tem), (g, l) subhumid Mediterranean (shMed), and (h, m) semiarid Mediterranean (saMed) ecoregions. Purple vertical lines represent the relative proportion of lateral water flux at each depth along the profiles (i.e., dominant source layer, DSL, curves) and shaded areas delimitate the DSL_{90} (riparian zone depth range contributing 90% of the total lateral water flux) for the available stream discharge dates in each case. Note that the information regarding the DSL is equivalent in both the upper DOC panels and the corresponding lower $N–NO_3^-$ panels. Note also that the scales of the *x*-axis are the same for the solute concentrations as well as for the relative proportion of later water flow (which ranges from 0% to 10% in all cases and it is not explicitly shown).

locations (Werner et al., 2021). Marked small-scale topographic variabilities are present in riparian zones in other temperate sites and therefore, a similar heterogeneous pattern likely emerges across this ecoregion (Blaurock et al., 2022; Frei et al., 2010).

The shape of the DSL curve and the segmented DSL_{90} in the Mediterranean sites indicate a more complex hydrological pattern (Figures 4g and 4h): within a single profile, upper riparian layers are hydrologically activated only sporadically but have a relatively large influence on the overall water flux. For example, at the subhumid site, depths above the median DSL_{90} (103 cm b.s.s.) were active only 1.5% of the time, but amounted to as much as 21% of the total lateral water flux (Figure S2 in Supporting Information S1). The pattern was similar at the semiarid site, where the activation of layers above the median DSL_{90} (47 cm b.s.s.) represented 0.8% of the time and accounted for 38% of the total lateral water flux (Figure S2 in Supporting Information S1). As a result, the DSL_{90} was 46 cm thick at the subhumid site and 86 cm thick at the semiarid site, both appreciably thicker than at the temperate and boreal profiles (Figure 4).

The difference between the two Mediterranean sites lies in the different *k* coefficients during high flow conditions, which was two times larger at the semiarid site. Consequently, lateral water fluxes were seemingly deeper and more restricted in space at the subhumid site. Nevertheless, we note that the riparian groundwater table–stream discharge relationship and the derived DSL at the semiarid site considered only the periods when the stream flowed. During the periods when there is no stream discharge and there is a hydrological disconnection between the riparian zone and stream, the riparian groundwater table at the semiarid Mediterranean site is located consistently below 200 cm b.s.s. (Butturini et al., 2003).

3.3. Riparian Zone DOC and N–NO_3^- Biogeochemistry

In general, both DOC and N–NO_3^- concentrations in riparian soil water were higher closer to the surface at the four sites (Figure 4). This spatial trend has been commonly observed for DOC in forest riparian zones across different regions (Sanderman et al., 2009; Schwab et al., 2018; Stewart et al., 2022), as well as for N–NO_3^-, although less information is available (but see Ranalli & Macalady, 2010). There were exceptions to this observation; for example, the wet profile at the temperate site showed increasing DOC concentrations with depth (Figure 4f) and no spatial trend for N–NO_3^- (Figure 4k), likely related to the nearly permanent saturated conditions. However, measuring chemistry at only two depths in this profile limits our ability to fully describe vertical patterns.

Accumulation and solubilization of organic matter and low mineralization rates due to hypoxic conditions driven by high moisture are likely behind the high DOC concentrations of the boreal riparian profiles (median value per depth varying between 15 and 71 mg L^{-1}; Figures 4a–4d) (Ledesma, Futter, et al., 2018). The dry location at the temperate site (Figure 4e) tended to exhibit lower DOC concentrations in soil water (median values per depth varying between 1.7 and 6.0 mg L^{-1}) than the wet location (Figure 4f), where median values per depth varied between 7.7 and 21.0 mg L^{-1}. This difference is also likely explained by greater accumulation and solubilization of organic matter in areas with high TWI, where persistently water-saturated conditions result in lower rates of organic matter decomposition and mineralization compared to areas with low TWI (Werner et al., 2021).

However, DOC concentrations at the boreal profiles were still distinctly higher than those at the wet temperate profile (Figures 4a–4f). Reasons behind this observation potentially include a (a) higher and more aromatic dissolved organic matter production in the coniferous trees and peat mosses of the boreal site than in the grasses present at the riparian zone of the temperate site (Borken et al., 2011; Hedwall & Mikusiński, 2016; Jones et al., 2014; Wania et al., 2009), (b) lower mineralization in the boreal site due to lower temperatures, and (c) higher solubility of dissolved organic matter in the boreal region due lower atmospheric nitrogen deposition (Dentener et al., 2006; Musolff et al., 2017).

Interestingly, the Mediterranean sites showed high DOC concentrations in upper and intermediate riparian depths (Figures 4g and 4h) despite their low soil organic carbon content (below 2%; Figure S3 in Supporting Information S1). At the subhumid site, the median DOC concentrations at 45 cm b.s.s. was 44 mg L^{-1}, whereas this metric reached 55 mg L^{-1} at 30 cm b.s.s. in the semiarid site. These concentrations are similar to the high concentrations measured in the shallow depths of the boreal profiles, where the soil organic carbon content is one order of magnitude higher, ranging between ca. 20% and 50% (Ledesma et al., 2015; Ledesma, Kothawala, et al., 2018). Thus, high DOC concentrations in riparian soil water can be found in contrasting ecoregions with markedly different conditions and soil organic carbon contents.

At the Mediterranean sites, the conditions that potentially favor high riparian soil solution DOC include high temperature for most of the year and sufficient soil moisture, both promoting microbial activity that releases DOC from organic matter decomposition (Kalbitz et al., 2000). At the semiarid site, for instance, our riparian soil moisture measurements (Text S1 in Supporting Information S1) showed values consistently higher than 10% with a median of ca. 20% at 20–50 cm b.s.s. during 2021 and 2022 (unpublished data). The high presence of roots observed in riparian soils at 30–45 cm b.s.s. at both sites can also potentially provide substantial amounts of exudate-derived DOC (Ledesma, Ruiz-Pérez, et al., 2021; Wen et al., 2020). Furthermore, accumulation of DOC during periods of low hydrological connection to the stream can also contribute to increase DOC concentrations in the soil solution pool (e.g., Harms & Grimm, 2010).

Riparian N–NO_3^- concentrations were relatively constant and extremely low in the boreal site (<0.01 mg L^{-1}; Figure 4i), which is coherent with the widespread high nitrogen limitation and low rates of net mineralization and nitrification reported for boreal soils (Sponseller et al., 2016). The wet profile of the temperate site also showed low and stable N–NO_3^- concentrations (ca. 0.05 mg L^{-1}; Figure 4k). Classically, wet-related hypoxic conditions in forest riparian zones in boreal and temperate regions favor denitrification and thus limit the production and mobilization of N–NO_3^- (Blackburn et al., 2017; Cirmo & McDonnell, 1997).

Conversely, N–NO_3^- concentrations in the dry temperate profile tended to be higher and more variable (Figure 4j), especially in the upper 10 cm b.s.s. layer (median = 0.4 mg L^{-1}), which was saturated <5% of the studied time (Figure S2 in Supporting Information S1). Notably, riparian N–NO_3^- concentrations were up to three orders of magnitude larger in the Mediterranean profiles (median value per depth varying between 0.2 and 14 mg L^{-1}; Figures 4l and 4m) compared to the boreal profiles. Concentrations were especially high and markedly variable in the upper aerated layers. In contrast to other ecoregions, net nitrification driven by high temperatures and sufficient soil moisture can lead to high and variable N–NO_3^- concentrations in riparian zones of Mediterranean catchments (Lupon, Sabater, et al., 2016; Pinay et al., 2018).

3.4. Riparian Zone Controls on Stream Chemistry

3.4.1. Stream Chemical Dynamics as a Function of Flow Conditions and Riparian Hydrological Connection

In general, stream DOC concentrations increased with increasing discharge, but this pattern was not consistent across discharge quartiles and ecoregions (Figure 5). In the boreal stream, DOC concentrations significantly increased from low- and intermediate-low flow conditions (quartiles Q1 and Q2) to intermediate-high flow conditions (quartile Q3), and from those to high flow conditions (quartile Q4) (Figure 5a). This result is consistent with stream discharge being a good predictor of stream DOC concentrations across the boreal region (Winterdahl et al., 2014). By contrast, no significant differences in DOC concentrations among discharge quartiles were revealed at the temperate stream (except for lower concentrations during low flow conditions, Figure 5c). However, this result is not inconsistent with the observation that stream DOC concentrations generally increase during individual storm events in ours and other temperate forest streams, likely because pulling the whole time series together masks the effect of seasonality (i.e., temperature-driven DOC variability), which exerts a strong influence on the concentration magnitude in this ecoregion (Musolff et al., 2018, 2021; Werner et al., 2019).

The two Mediterranean streams showed apparent increases in DOC concentrations from low to high discharge quartiles (Figures 5e and 5g), but the low sample size precluded a statistically significant result. Indeed, a simple linear regression between stream discharge and DOC concentration was significantly positive at both sites ($R^2 = 0.13$, $p < 0.05$ at the subhumid site; $R^2 = 0.22$, $p < 0.05$ at the semiarid site; Figure S4 in Supporting Information S1). Previous studies have also shown that DOC concentrations increase during storm events (which are more common in autumn and winter) at both streams (Bernal et al., 2002; Ledesma et al., 2022).

Stream N–NO_3^- concentrations also generally increased with increasing discharge, but the results were mixed across ecoregions (Figure 5). For instance, concentrations at the boreal stream were consistently low and independent of flow conditions (Figure 5b), a pattern that has been observed in ours and other boreal forest headwaters due to nitrogen limitation (Blackburn et al., 2017; Löfgren et al., 2011; Luke et al., 2007). At the temperate stream, we observed an apparent increase in N–NO_3^- concentrations with discharge supported by linear regression ($R^2 = 0.30$, $p < 0.0001$; Figure S4 in Supporting Information S1), although differences were only statistically significant between discharge quartiles Q2 and Q4 (Figure 5d). In other temperate forest headwaters, patterns are not uniform, but observations generally show increasing N–NO_3^- concentrations with discharge (Cirmo & McDonnell, 1997).

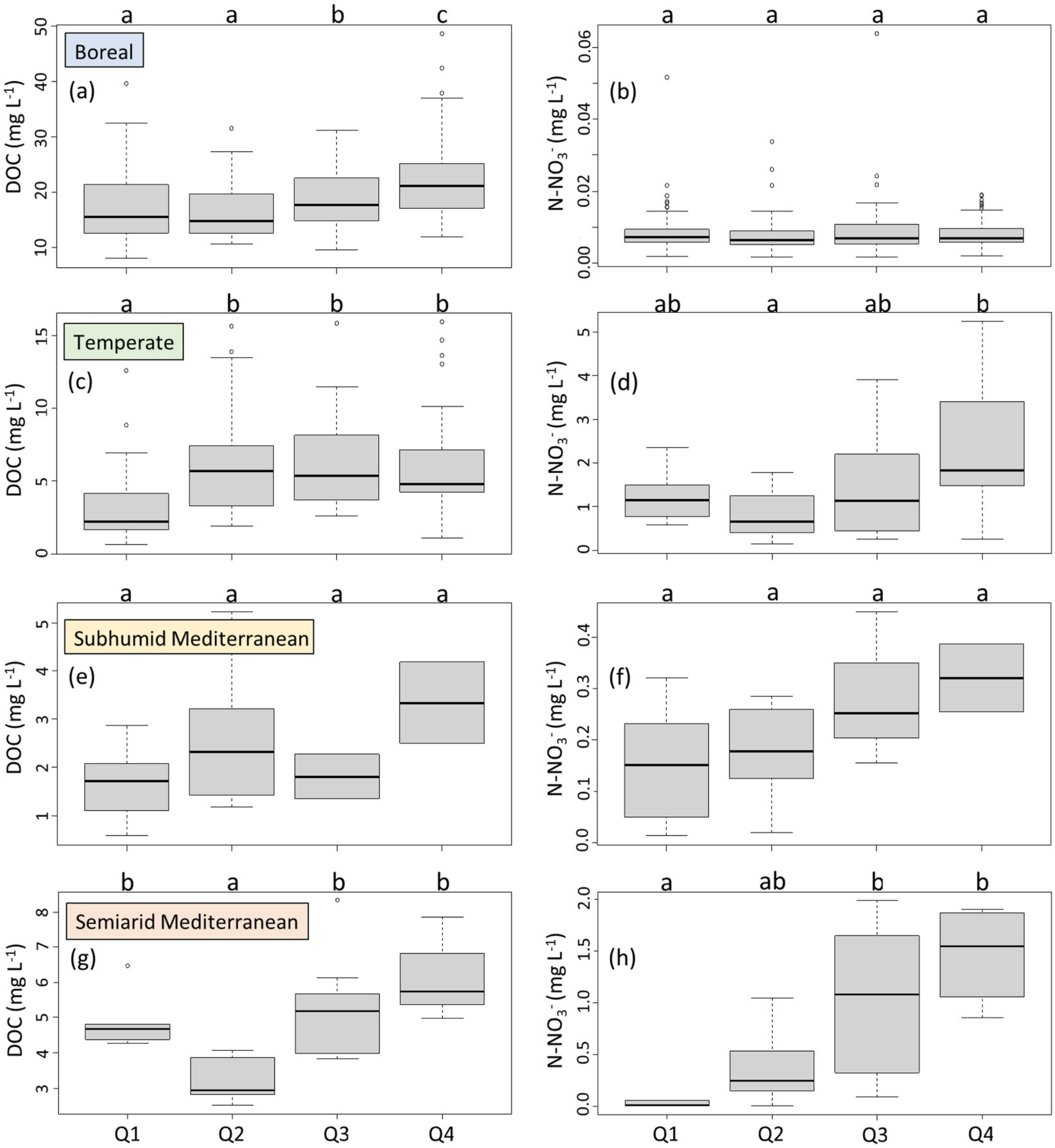

Figure 5. Box plots of available dissolved organic carbon (DOC, left-side panels) and nitrate ($N–NO_3^-$, right-side panels) concentrations in (a–b) boreal, (c–d) temperate, (e–f) subhumid Mediterranean, and (g–h) semiarid Mediterranean streams. For each ecoregion, data are grouped by stream discharge quartiles (Q1 to Q4). Statistical differences using the Kruskal-Wallis test followed by a post hoc Dunn's test for pair comparisons are denoted with letters. Note that the scales of the *y*-axis differ across panels.

At the Mediterranean streams, $N–NO_3^-$ concentrations systematically increase with discharge, but again, the low sample size only produced statistically significant differences between Q1 and Q3–Q4 at the semiarid site (Figures 5f and 5h). Nevertheless, the apparent increases in concentrations with discharge were supported by linear regression ($R^2 = 0.27$, $p < 0.005$ at the subhumid site; $R^2 = 0.34$, $p < 0.005$ at the semiarid site; Figure S4 in Supporting Information S1). Concentrations of $N–NO_3^-$ are generally higher during storm flow than during base flow in ours and other Mediterranean forest headwaters (Àvila et al., 1992; Bernal et al., 2002; Ledesma et al., 2022).

According to the DSL framework, the observed variability in stream solute concentrations with discharge can result from the activation of different riparian soil layers with distinct chemistry during different flow conditions (Seibert et al., 2009). Riparian DOC at the boreal and Mediterranean profiles (Figures 4a–4d and 4g–4h) and $N–NO_3^-$ at the temperate dry and Mediterranean profiles (Figures 4j, 4l and 4m) generally increase in the upper layers of the corresponding DSL_{90}. These upper riparian layers with higher concentrations are typically hydrologically activated and connected to the stream during higher flow conditions, which can explain the higher stream concentrations observed for these two solutes when the discharge increases (Figures 5a, 5d and 5e–5h). Likewise, the lack of variability in stream $N{-}NO_3^-$ concentrations with flow conditions in the boreal site (Figure 5b) can be related to the vertically stable $N{-}NO_3^-$ concentrations in the DSL_{90} (Figure 4i). Finally, the small variation in stream DOC with discharge at the temperate site (Figure 5c) may be explained by the divergent DOC vertical patterns observed at the dry and wet areas in the riparian zone (Figures 4e and 4f).

3.4.2. Does Stream Chemistry Entirely Reflect Riparian Soil Water Chemistry?

The simple qualitative assessment presented in the previous section supports the paradigm that stream chemical dynamics can be driven by vertical patterns in riparian soil water chemistry across varying flow conditions, and thus the hypothesis that stream water chemistry mirrors riparian soil water chemistry (Bishop et al., 2004; Stewart et al., 2022). However, it does not provide a quantitative resolution of the relative importance of riparian zones in controlling stream chemistry. In this section, we shed light on this question by using the DSL framework to explore the level of correspondence between stream and riparian soil water chemistry. We compared DOC and $N{-}NO_3^-$ concentrations in the stream with corresponding flow-weighted concentrations from the riparian zone in our four forest headwater catchments (Figure 6). We separated the comparison by stream discharge quartiles because the riparian-stream correspondence based on DSL assumptions might depend on flow conditions. Specifically, varying flow conditions could potentially trigger the activation of catchment compartments other than the riparian zone, as well as control stream water residence times and therefore in-stream biogeochemical processing (Li et al., 2021; Zimmer & McGlynn, 2018).

One of the most striking patterns observed was the consistently lower DOC concentrations in the stream compared to the estimated DOC flow-weighted concentration exported from the riparian zone at the boreal site (Figure 6a). This pattern holds true for the four representative profiles presented here and across all flow conditions. Dilution from sources other than the riparian zone is unlikely to explain this result because a combination of isotopic, hydrological, and modeling approaches suggests that there is limited bypass of water below 100 cm b.s.s. in this riparian zone (Amvrosiadi et al., 2017; Peralta-Tapia et al., 2015). Rapid in-stream uptake of DOC can partially explain the discrepancy because this process has been observed in other streams in the Krycklan catchment (Lupon et al., 2023). However, it is unlikely that in-stream DOC uptake alone can account for such DOC removal (>10 mg L^{-1}), given that the dissolved organic matter mobilized from riparian zones is largely non-labile and water residence times are short (Berggren et al., 2023; Kothawala et al., 2015; Ledesma, Kothawala, et al., 2018).

We hypothesize that the main process removing DOC from this boreal stream is rapid flocculation and co-precipitation of DOC with iron (Fe) once hypoxic riparian zone water meets oxic conditions in the stream (Einarsdóttir et al., 2020; Knorr, 2013; Riedel et al., 2013; Tittel et al., 2022). The generally wet and therefore reducing conditions of the riparian zone, together with the very low concentration of $N{-}NO_3^-$ as a competing electron acceptor, would favor the formation of soluble Fe^{2+} (Tittel et al., 2022). Indeed, soil water in the four boreal riparian profiles showed high concentrations of total Fe that varied from 1 to as much as 15 mg L^{-1} (Figure S5 in Supporting Information S1). To put it in context, the concentration of total Fe in riparian soil water at the Mediterranean sites was in the order of 0.001–0.1 mg L^{-1} (Figure S5 in Supporting Information S1). Hence, we hypothesize that reduced Fe^{2+} from the riparian zone can be quickly oxidized in the boreal stream into Fe^{3+} and removed from the water column together with affinitive compounds such as DOC via precipitation of Fe hydroxides (Neubauer et al., 2013; Riedel et al., 2013). This process is further supported by the significantly lower Fe concentrations found in stream water compared to riparian soil water across the bigger Krycklan catchment (Köhler et al., 2014; Lidman et al., 2017; Škerlep et al., 2023), and likely present across the boreal ecoregion.

The same mechanism can be invoked to explain the higher DOC flow-weighted concentration in the wet riparian profile of the temperate site compared to the stream concentration, particularly during lower flow conditions (Figure 6c). Median soil water Fe concentrations in this profile were 12.2 and 18.0 mg L^{-1} at 15 and 30 cm b.s.s., respectively (Figure S5 in Supporting Information S1). During low flow conditions, the DSL_{90} of the wet profile ranged from 15 to 37 cm b.s.s., implying a hydrological connection between these soil solution Fe-rich riparian layers and the stream. During higher flow conditions, saturation-excess overland flow increasingly gains importance as the mode of water export from the high TWI zones here (Werner et al., 2021). Under these

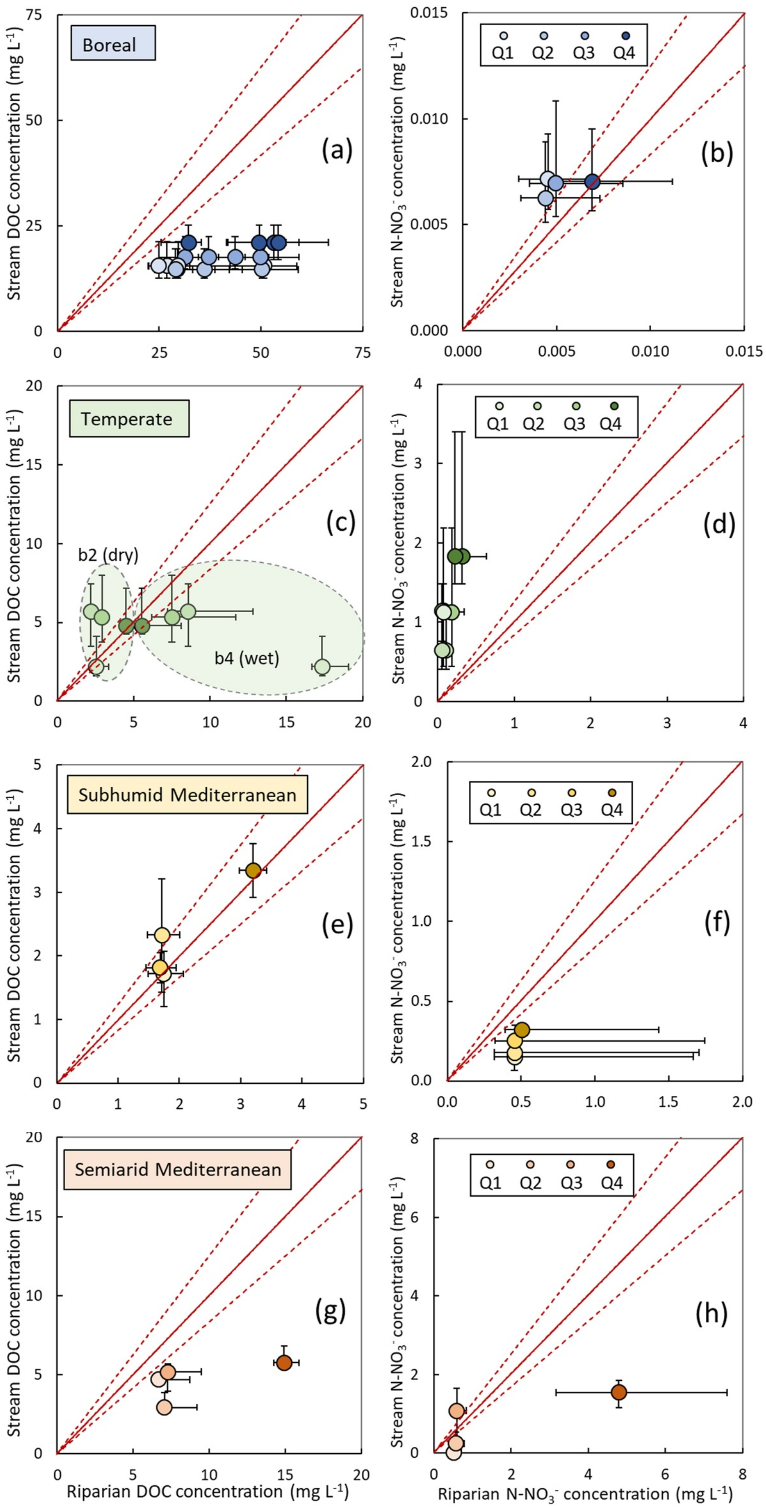

Figure 6. Relationships between concentrations of dissolved organic carbon (DOC, left-side panels) and nitrate ($N–NO_3^-$, right-side panels) in streams and corresponding flow-weighted concentrations in the associated riparian zone profiles in (a–b) boreal, (c–d) temperate, (e–f) subhumid Mediterranean, and (g–h) semiarid Mediterranean sites. For each ecoregion, data are grouped by discharge quartiles (Q1 to Q4). Circles are medians and error bars represent interquartile ranges. The 1:1 line is indicated by a red line, together with ±20% uncertainty bands as dashed red lines. Note that panel (a) contains four sets of data from four riparian profiles. Similarly, panels (c–d) contain two sets of data from two riparian profiles.

circumstances, stream Fe-DOC co-precipitation likely diminishes in importance because Fe oxidation can occur as water moves overland in the riparian zone. Indeed, the overall DSL_{90} of the wet profile ranged from 8 cm b.s.s. to 11 cm above the soil surface, highlighting the importance of flow paths overland in the wet areas. By contrast, soil water Fe concentrations were markedly lower at the dry riparian profile (ranging from 0.02 to 0.08 mg L^{-1} at 15 and 30 cm b.s.s.), where the DOC flow-weighted concentration tended to be similar to the stream concentrations at both low and high flow conditions (Figure 6c).

At the temperate site, we also observed a discrepancy between riparian and stream $N–NO_3^-$, whereby stream concentrations are considerably higher than those expected from riparian zone lateral fluxes, especially during high flow conditions and independently of riparian TWI (Figure 6d). The most feasible explanation for this discrepancy is the contribution of additional sources of water with high $N–NO_3^-$ concentrations. Specifically, we hypothesized that the recurrent water ponds over the riparian soil surface observed at this and similar temperate forest headwater catchments might play an important role in this context (Blaurock et al., 2022; Werner et al., 2021). We measured a median $N–NO_3^-$ concentration as high as 8.4 mg L^{-1} (interquartile range = 7.0–10.2 mg L^{-1}, $N = 8$) in water sampled from these ponds during a 3-month survey in 2023 (DOC concentrations were similar to those found in the stream).

The contribution of the ponds to the stream when they become hydrologically connected via overland flow, especially during higher flow conditions, is difficult to quantify. However, this contribution is potentially significant in terms of $N–NO_3^-$ given the discrepancy between riparian and stream $N–NO_3^-$ based on the DSL calculations, which did not account for the ponds. The high levels of $N–NO_3^-$ in the ponds could be related to the upslope forest dieback caused by the bark beetle infestation that followed a 2-year drought period starting in 2018, as we have recently suggested elsewhere (Musolff et al., 2024). Tree death and subsequent removal potentially had two main effects: (a) the hydrological effect of decreasing evapotranspiration and (b) the biogeochemical effect of reducing nutrient uptake (Hope, 2009; Kreutzweiser et al., 2008). As a consequence, relatively more water with high levels of organic and inorganic nitrogen (especially the more mobile $N–NO_3^-$) could begin to mobilize from the upslope into the riparian zone, where we hypothesized it emerged into the ponds due to upwelling at the edge of the riparian zone. Indeed, considering only the early data period before the dieback (2013–2014; Table 2), the discrepancy between stream and riparian zone $N–NO_3^-$ was notably smaller (Figure S6 in Supporting Information S1). This finding suggests that, before the drought, pond water was either less important in contributing to the stream or had lower $N–NO_3^-$ concentrations. Pond water could potentially be integrated in future studies within the DSL framework via characterization of its hydrological transfer to the stream and regular monitoring of its chemistry.

The last clear discrepancy between riparian and stream chemistry was observed at the Mediterranean semiarid site, where both stream DOC and $N–NO_3^-$ concentrations were lower than those expected from riparian zone lateral fluxes, especially during high flow conditions (Figures 6g and 6h). This catchment is larger and the soils are notably deeper than those in the boreal and temperate sites, which opens the door to potential inflows of deep groundwater with a distinct chemical signal to the stream bypassing the riparian zone. Indeed, the median DOC and $N–NO_3^-$ concentrations from the deep well near the valley bottom of the catchment (which we assume represents deep groundwater) were, respectively, 2.5 and 0.02 mg L^{-1}, notably lower than stream and riparian DOC and $N–NO_3^-$ concentrations (Figures 6g and 6h). This deep groundwater flows through a medium of very low hydraulic conductivity and remains hydrologically disconnected from the stream for large parts of the year, that is, when there is no stream flow or this is in recession (Butturini et al., 2003). Nevertheless, it could dilute the riparian DOC and $N–NO_3^-$ signal during high flows, largely explaining the notably lower DOC and $N–NO_3^-$ concentrations in the stream compared to the riparian zone at the semiarid site.

For the remaining comparisons, including the previously mentioned correspondence between the dry riparian profile and stream for DOC at the temperate site, the chemistry of riparian and stream waters was either similar or exhibited small differences (Figures 6b, 6e, and 6f). Riparian spatial heterogeneity can potentially explain these smaller discrepancies (Stewart et al., 2022). Hydrological and biogeochemical variations within the riparian zone can complicate the collection of representative riparian soil water samples, underscoring the importance of selecting representative sampling profiles, which we ensured through careful selection at our sites.

In turn, in-stream biological processes could also modulate the riparian DOC and $N–NO_3^-$ signals in some cases. For instance, net nitrification has been observed in the Krycklan catchment during lower flow conditions (Lupon et al., 2020), and could have contributed to the apparently higher stream $N–NO_3^-$ concentrations compared to the riparian zone at the boreal site during low flow (Figure 6b). The prevalence of in-stream N–NO_3^- uptake in the Mediterranean streams, especially during low flow conditions (Bernal et al., 2012), could have contributed to the apparently lower stream N–NO_3^- concentrations compared to those expected from riparian inputs (Figures 6f and 6h). In-stream DOC uptake can be quantitatively important in Mediterranean streams because of its labile character, which favors rapid assimilation even during periods of short water residence times (Bernal et al., 2019). This process is potentially more prominent in semiarid systems (Catalán et al., 2018), and could have contributed to the discrepancy between riparian and stream DOC at our site (Figure 6g). Ultimately, the complex equilibrium among supply, demand, and in-stream uptake, together with the variability in metabolically favorable stoichiometric C:N ratios, can regulate in-stream heterotrophic processes, especially at the Mediterranean sites (Bernal et al., 2019; Peñarroya et al., 2023).

3.5. Conceptualization of the DSL and Riparian-Stream Linkages Across Ecoregions

We found that the DSL that contributes the most to water and solute fluxes to the stream (Figure 4) is shallower and thinner in boreal systems due to both geological and soil characteristics (shallow glacial till, high organic matter content, low bulk density, and large structural pores) and overall wetness (Figure 7). In the more mineral riparian zones of temperate systems, the DSL size and position depend on TWI areas defined by small-scale topographic heterogeneity: the DSL of high TWI areas resembles that of boreal sites, whereas the DSL of low TWI areas is wider and deeper (Figure 7). In Mediterranean sites, the DSL is notably deeper than at boreal and temperate sites, but upper riparian layers that are hydrologically activated only sporadically can have a relatively large influence on the overall water and solute flux (Figure 7), especially in semiarid systems (Figure 4). This pattern is driven by large precipitation events characteristic of Mediterranean regions.

Riparian DOC concentrations can be high under contrasting conditions (Figures 4 and 7): cold and moist favoring low mineralization and accumulation of organic matter (e.g., boreal site), and warm and relatively dry promoting microbial activity and DOC release in the root zone (e.g., upper riparian layers of Mediterranean sites). Riparian N–NO_3^- appears to be clearly driven by the redox state, whereby wet-related hypoxic conditions favor denitrification and low concentrations (boreal and temperate sites) and oxic conditions favor nitrification and high concentrations (Mediterranean sites).

We showed that the position of the DSL can be broadly linked to stream chemical dynamics across all ecoregions via the activation of different riparian soil layers with distinct chemistry during different flow conditions (Figures 4 and 5). This assessment supports previous conceptualizations on which the DSL framework is based (Bishop et al., 2004), as well as the broad concepts of for example, the shallow and deep hypothesis, which suggests that stream water chemistry is shaped by distinct source waters from different depths (Stewart et al., 2022).

However, when exploring the correspondence between stream chemistry and that expected from riparian inputs, discrepancies emerged (Figure 6). In some cases, the discrepancies could be attributed to varying contributions from water sources other than the riparian zone, which are a function of temporal variability in catchment hydrological connectivity. Our assessment helped hypothesizing the origin of these sources, including deep groundwater (e.g., Mediterranean ecoregion) and pond water overland (e.g., temperate ecoregion) (Figure 7). In other cases, the observed discrepancies could be better explained by in-stream biogeochemical processes, including geochemical precipitation (e.g., boreal and temperate ecoregions) and biological uptake or release (universal, but likely more relevant in the Mediterranean ecoregion) (Figure 7). In summary, the significance of (a) water sources other than the riparian zone and (b) in-stream biogeochemical processes can vary across flow conditions and ecoregions, but our results indicate that they can be large enough to modulate the riparian zone chemical signal that is subsequently reflected in the stream (Figure 7).

4. Concluding Remarks and Implications for Future Research

Riparian zones in forest headwaters exhibit unique hydrological behavior and biogeochemistry relative to the rest of the catchment, and exert a pivotal role in determining stream water chemistry. This study delves into these unique characteristics and their differences across four ecoregions in Europe: boreal, temperate, subhumid Mediterranean, and semiarid Mediterranean. Using DOC and N–NO_3^- as illustrative examples, this study also sheds light on the relative importance of the riparian zone in determining stream chemistry.

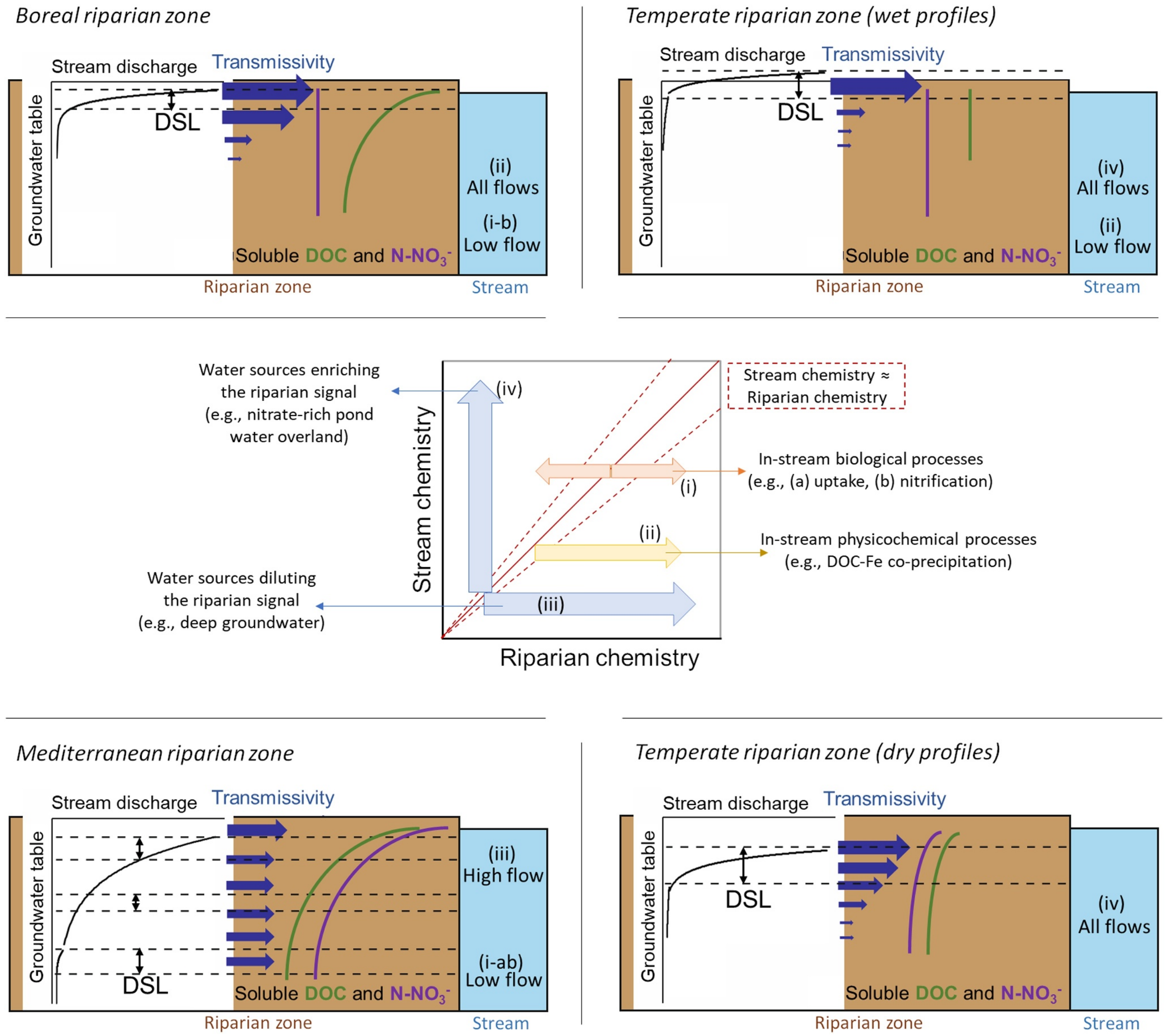

Figure 7. Conceptual figure summarizing our results and proposed hypotheses for the studied ecoregions. For a typical temperate forest headwater catchment, we separate wet from dry profiles, while both subhumid and semiarid Mediterranean cases are integrated together. The dominant source layer (DSL, delimited by dashed horizontal lines) is the riparian zone depth stratum through which most of the water and solutes are supplied to streams and is derived from the relationship between the riparian groundwater table and stream discharge. The lateral transmissivity along the profile is based on this relationship and is illustrated with blue arrows, where larger arrows represent greater transmissivity. Archetypical mean dissolved organic carbon (DOC) and nitrate ($N–NO_3^-$) concentration profiles in the riparian soil solution are presented as green and purple lines, respectively. The central panel illustrates potential mechanisms by which stream chemistry may deviate from riparian soil chemistry. Roman numerals in the blue box representing the stream indicate which ecoregion these processes might be associated with, and whether they dominate during high flow, low flow, or across various flow conditions.

We note that our riparian-stream comparison is limited by riparian heterogeneity and does not provide definitive answers but hypotheses that should be tested in future studies. Regardless, we conclude that streams do not always mirror the chemistry of soil water in distinct riparian layers. Therefore, the connection between riparian and stream chemistry might not be as straightforward as previously stated (e.g., Ledesma, Kothawala, et al., 2018), and neither can stream chemistry simply be described by a mixture of water sources (e.g., Easthouse et al., 1992; Inamdar & Mitchell, 2006; Stewart et al., 2022).

It is open to investigation how the hydrological and biogeochemical behavior of riparian zones and their link to stream chemistry will be altered under the influence of a changing climate. A “mediterranization” of the temperate

10.1029/2024GB008250

and boreal climates, that is, an increase in the frequency and severity of extreme events such as droughts and large storms, is ongoing and predicted to accentuate (Rädler et al., 2019; Spinoni et al., 2018). However, the long-term factors that shaped the distinct geology, soil characteristics, and vegetation across these different ecoregions make it difficult to foresee a "mediterranization" of the riparian and stream responses at more northern latitudes. This is well-exemplified here by how our temperate catchment responded to a drought. The vegetation that evolved in this site could not cope with this extreme event, and by dying, likely triggered hydrological (i.e., lower evapotranspiration) and biogeochemical (i.e., reduced nutrient uptake) processes that are not seen in Mediterranean sites after droughts as the vegetation there are adapted to withstand such events. This drought-induced tree death manifested in large parts of Central Europe and is a present reality and a future threat across temperate forest catchments (Romeiro et al., 2022).

We highlight that multiple-site approaches can help identify common patterns and specific differences in riparian hydrological and biogeochemical characteristics across ecoregions, as well as the factors driving these patterns and the resulting dynamics of stream water chemistry. This comprehensive empirical and conceptual synthesis of our fundamental understanding of processes controlling water transfer and solute transformation and mobilization between riparian zones and streams based on the DSL framework can support both scientific assessments and management of river networks.

Data Availability Statement

The Krycklan data used in the study are available at SITES via https://data.fieldsites.se/portal/ with a Creative Commons by Attribution licence (CCBY). The Rappbode, Font del Regàs, and Fuirosos data are available at the research data repository HydroShare, also with a CCBY licence (Ledesma, 2025).

Acknowledgments

This work was supported by the project RIPARIONS granted to JLJL by the European Commission through a Marie Skłodowska Curie Individual Fellowship (H2020-MSCA-IF-2018-834363). AL was supported by the projects INHOT (CNS2022-135690) and FLUPRINT (EUR2023-143456) from the Spanish Ministry of Science, Innovation, and Universities, AEI/FEDER UE, and Next Generation funding. SB was supported by the projects EVASIONA (PID2021-122817-NB-100) and RIPAMED (CNS2023-144737) from the Spanish Ministry of Science, Innovation, and Universities, AEI/FEDER UE, and Next Generation funding. CJ was supported by an FPU fellowship (FPU21/03523) from the Spanish Ministry of Science, Innovation, and Universities. We would like to thank Tejshree Tiwari, Johannes Tiwari, and Kim Lindgren for assistance with the Krycklan database; Toralf Keller for invaluable work in the field, lab, and data pre-processing at the Rappbode catchment; and Montserrat Soler for pre-processing of the data from Font del Regàs and Fuirosos. The Matlab scripts used to compute most of the calculations in this study were prepared with the assistance of ChatGPT. Finally, we would like to thank two anonymous reviewers, as well as the Editor-in-Chief and Associate Editor who handled the manuscript, for valuable comments that improved the quality of this work. Open Access funding enabled and organized by Projekt DEAL.

References

Amvrosiadi, N., Bishop, K., & Seibert, J. (2017). Soil moisture storage estimation based on steady vertical fluxes under equilibrium. *Journal of Hydrology*, *553*, 798–804. https://doi.org/10.1016/j.jhydrol.2017.08.042

Àvila, A., Piñol, J., Rodà, F., & Neal, C. (1992). Storm solute behavior in a montane Mediterranean forested catchment. *Journal of Hydrology*, *140*(1–4), 143–161. https://doi.org/10.1016/0022-1694(92)90238-q

Battin, T. J., Lauerwald, R., Bernhardt, E. S., Bertuzzo, E., Gómez-Gener, L., Hall, R., et al. (2023). River ecosystem metabolism and carbon biogeochemistry in a changing world. *Nature*, *613*(7944), 449–459. https://doi.org/10.1038/s41586-022-05500-8

Benstead, J. P., & Leigh, D. S. (2012). An expanded role for river networks. *Nature Geoscience*, *5*(10), 678–679. https://doi.org/10.1038/ngeo1593

Berggren, M., Ye, L. L., Sponseller, R. A., Bergström, A. K., Karlsson, J., Verheijen, H., & Hensgens, G. (2023). Nutrient limitation masks the dissolved organic matter composition effects on bacterial metabolism in unproductive freshwaters. *Limnology & Oceanography*, *68*(9), 2059–2069. https://doi.org/10.1002/lno.12406

Bergknut, M., Meijer, S., Halsall, C., Ågren, A., Laudon, H., Köhler, S., et al. (2010). Modelling the fate of hydrophobic organic contaminants in a boreal forest catchment: A cross disciplinary approach to assessing diffuse pollution to surface waters. *Environmental Pollution*, *158*(9), 2964–2969. https://doi.org/10.1016/j.envpol.2010.05.027

Bernal, S., Butturini, A., & Sabater, F. (2002). Variability of DOC and nitrate responses to storms in a small Mediterranean forested catchment. *Hydrology and Earth System Sciences*, *6*(6), 1031–1041. https://doi.org/10.5194/hess-6-1031-2002

Bernal, S., Butturini, A., & Sabater, F. (2005). Seasonal variations of dissolved nitrogen and DOC: DON ratios in an intermittent mediterranean stream. *Biogeochemistry*, *75*(2), 351–372. https://doi.org/10.1007/s10533-005-1246-7

Bernal, S., Lupon, A., Ribot, M., Sabater, F., & Martí, E. (2015). Riparian and in-stream controls on nutrient concentrations and fluxes in a headwater forested stream. *Biogeosciences*, *12*(6), 1941–1954. https://doi.org/10.5194/bg-12-1941-2015

Bernal, S., Lupon, A., Wollheim, W. M., Sabater, F., Poblador, S., & Martí, E. (2019). Supply, demand, and in-stream retention of dissolved organic carbon and nitrate during storms in mediterranean forested headwater streams. *Frontiers in Environmental Science*, *7*, 60. https://doi.org/10.3389/fenvs.2019.00060

Bernal, S., von Schiller, D., Martí, E., & Sabater, F. (2012). In-stream net uptake regulates inorganic nitrogen export from catchments under base flow conditions. *Journal of Geophysical Research*, *117*(G3), G00N05. https://doi.org/10.1029/2012jg001985

Bernal, S., von Schiller, D., Sabater, F., & Martí, E. (2013). Hydrological extremes modulate nutrient dynamics in Mediterranean climate streams across different spatial scales. *Hydrobiologia*, *719*(1), 31–42. https://doi.org/10.1007/s10750-012-1246-2

Bernhardt, E. S., Blaszczak, J. R., Ficken, C. D., Fork, M. L., Kaiser, K. E., & Seybold, E. C. (2017). Control points in ecosystems: Moving beyond the hot spot hot moment concept. *Ecosystems*, *20*(4), 665–682. https://doi.org/10.1007/s10021-016-0103-y

Bishop, K., Seibert, J., Köhler, S., & Laudon, H. (2004). Resolving the Double Paradox of rapidly mobilized old water with highly variable responses in runoff chemistry. *Hydrological Processes*, *18*(1), 185–189. https://doi.org/10.1002/hyp.5209

Bishop, K. H., Grip, H., & O'Neill, A. (1990). The origins of acid runoff in a hillslope during storm events. *Journal of Hydrology*, *116*(1–4), 35–61. https://doi.org/10.1016/0022-1694(90)90114-d

Blackburn, M., Ledesma, J. L. J., Näsholm, T., Laudon, H., & Sponseller, R. A. (2017). Evaluating hillslope and riparian contributions to dissolved nitrogen (N) export from a boreal forest catchment. *Journal of Geophysical Research-Biogeosciences*, *122*(2), 324–339. https://doi.org/10.1002/2016jg003535

Blaurock, K., Garthen, P., da Silva, M. P., Beudert, B., Gilfedder, B. S., Fleckenstein, J. H., et al. (2022). Riparian microtopography affects event-driven stream DOC concentrations and DOM quality in a forested headwater catchment. *Journal of Geophysical Research-Biogeosciences*, *127*(12), e2022JG006831. https://doi.org/10.1029/2022jg006831

Borken, W., Ahrens, B., Schulz, C., & Zimmermann, L. (2011). Site-to-site variability and temporal trends of DOC concentrations and fluxes in temperate forest soils. *Global Change Biology*, *17*(7), 2428–2443. https://doi.org/10.1111/j.1365-2486.2011.02390.x

Budyko, M. I. (1974). *Climate and life* (Vol. 18). Academic Press.

Butturini, A. (2021). Fuirosos stream (NE Iberian Peninsula): For how much longer? *Limnética*, *40*(1), 205–222. https://doi.org/10.23818/limn.40.14

Butturini, A., Bernal, S., Nin, E., Hellin, C., Rivero, L., Sabater, S., & Sabater, F. (2003). Influences of the stream groundwater hydrology on nitrate concentration in unsaturated riparian area bounded by an intermittent Mediterranean stream. *Water Resources Research*, *39*(4), 1110. https://doi.org/10.1029/2001wr001260

Camargo, J. A., & Alonso, A. (2006). Ecological and toxicological effects of inorganic nitrogen pollution in aquatic ecosystems: A global assessment. *Environment International*, *32*(6), 831–849. https://doi.org/10.1016/j.envint.2006.05.002

Campbell, J. L., Rustad, L. E., Bailey, S. W., Bernhardt, E. S., Driscoll, C. T., Green, M. B., et al. (2021). Watershed studies at the Hubbard Brook Experimental Forest: Building on a long legacy of research with new approaches and sources of data. *Hydrological Processes*, *35*(1), e14016. https://doi.org/10.1002/hyp.14016

Catalán, N., Casas-Ruiz, J. P., Arce, M. I., Abril, M., Bravo, A. G., del Campo, R., et al. (2018). Behind the scenes: Mechanisms regulating climatic patterns of dissolved organic carbon uptake in headwater streams. *Global Biogeochemical Cycles*, *32*(10), 1528–1541. https://doi.org/10.1029/2018gb005919

Chow, A. T., Tanji, K. K., & Gao, S. D. (2003). Production of Dissolved Organic Carbon (DOC) and Trihalomethane (THM) precursor from peat soils. *Water Research*, *37*(18), 4475–4485. https://doi.org/10.1016/s0043-1354(03)00437-8

Cirmo, C. P., & McDonnell, J. J. (1997). Linking the hydrologic and biogeochemical controls of nitrogen transport in near-stream zones of temperate-forested catchments: A review. *Journal of Hydrology*, *199*(1–2), 88–120. https://doi.org/10.1016/s0022-1694(96)03286-6

Cole, J. J., Prairie, Y. T., Caraco, N. F., McDowell, W. H., Tranvik, L. J., Striegl, R. G., et al. (2007). Plumbing the global carbon cycle: Integrating inland waters into the terrestrial carbon budget. *Ecosystems*, *10*(1), 171–184. https://doi.org/10.1007/s10021-006-9013-8

Dentener, F., Drevet, J., Lamarque, J. F., Bey, I., Eickhout, B., Fiore, A. M., et al. (2006). Nitrogen and sulfur deposition on regional and global scales: A multimodel evaluation. *Global Biogeochemical Cycles*, *20*(4), GB4003. https://doi.org/10.1029/2005gb002672

Easthouse, K. B., Mulder, J., Christophersen, N., & Seip, H. M. (1992). Dissolved organic carbon fractions in soil and stream water during variable hydrological conditions at Birkenes, Southern Norway. *Water Resources Research*, *28*(6), 1585–1596. https://doi.org/10.1029/92wr00056

Einarsdóttir, K., Attermeyer, K., Hawkes, J. A., Kothawala, D., Sponseller, R. A., & Tranvik, L. J. (2020). Particles and aeration at mire-stream interfaces cause selective removal and modification of dissolved organic matter. *Journal of Geophysical Research-Biogeosciences*, *125*(12), e2020JG005654. https://doi.org/10.1029/2020jg005654

EMEP Status Report. (2023). *Transboundary particulate matter, photo-oxidants, acidifying and Eutrophying components*. Joint MSC-W & CCC & CEIP & CIAM Report.

Fovet, O., Ruiz, L., Hrachowitz, M., Faucheux, M., & Gascuel-Odoux, C. (2015). Hydrological hysteresis and its value for assessing process consistency in catchment conceptual models. *Hydrology and Earth System Sciences*, *19*(1), 105–123. https://doi.org/10.5194/hess-19-105-2015

Frei, S., Knorr, K. H., Peiffer, S., & Fleckenstein, J. H. (2012). Surface micro-topography causes hot spots of biogeochemical activity in wetland systems: A virtual modeling experiment. *Journal of Geophysical Research*, *117*(G4), G00N12. https://doi.org/10.1029/2012jg002012

Frei, S., Lischeid, G., & Fleckenstein, J. H. (2010). Effects of micro-topography on surface-subsurface exchange and runoff generation in a virtual riparian wetland—a modeling study. *Advances in Water Resources*, *33*(11), 1388–1401. https://doi.org/10.1016/j.advwatres.2010.07.006

Grabs, T., Bishop, K., Laudon, H., Lyon, S. W., & Seibert, J. (2012). Riparian zone hydrology and soil water Total Organic Carbon (TOC): Implications for spatial variability and upscaling of lateral riparian TOC exports. *Biogeosciences*, *9*(10), 3901–3916. https://doi.org/10.5194/bg-9-3901-2012

Gutierrez Lopez, J., Tor-Ngern, P., Oren, R., Kozii, N., Laudon, H., & Hasselquist, N. J. (2021). How tree species, tree size, and topographical location influenced tree transpiration in northern boreal forests during the historic 2018 drought. *Global Change Biology*, *27*(13), 3066–3078. https://doi.org/10.1111/gcb.15601

Harms, T. K., & Grimm, N. B. (2010). Influence of the hydrologic regime on resource availability in a semi-arid stream-riparian corridor. *Ecohydrology*, *3*(3), 349–359. https://doi.org/10.1002/eco.119

Hedwall, P. O., & Mikusiński, G. (2016). Sprucification in protected forests: Myth or veracity?—clues from 60 years survey data. *Applied Vegetation Science*, *19*(3), 371–380. https://doi.org/10.1111/avsc.12233

Hooper, R. P., Christophersen, N., & Peters, N. E. (1990). Modeling streamwater chemistry as a mixture of Soilwater end-members—An application to the Panola mountain catchment, Georgia, U.S.A. *Journal of Hydrology*, *116*(1–4), 321–343. https://doi.org/10.1016/0022-1694(90)90131-g

Hope, G. D. (2009). Clearcut harvesting effects on soil and creek inorganic nitrogen in high elevation forests of southern interior British Columbia. *Canadian Journal of Soil Science*, *89*(1), 35–44. https://doi.org/10.4141/cjss06032

Hruška, J., Kram, P., Moldan, F., Oulehle, F., Evans, C. D., Wright, R. F., et al. (2014). Changes in soil dissolved Organic Carbon affect reconstructed history and projected future trends in surface water acidification. *Water Air and Soil Pollution*, *225*(7), 2025. https://doi.org/10.1007/s11270-014-2015-9

Iavorivska, L., Boyer, E. W., & DeWalle, D. R. (2016). Atmospheric deposition of organic carbon via precipitation. *Atmospheric Environment*, *146*, 153–163. https://doi.org/10.1016/j.atmosenv.2016.06.006

Inamdar, S. P., & Mitchell, M. J. (2006). Hydrologic and topographic controls on storm-event exports of Dissolved Organic Carbon (DOC) and nitrate across catchment scales. *Water Resources Research*, *42*(3), W03421. https://doi.org/10.1029/2005wr004212

Jones, D. L., Simfukwe, P., Hill, P. W., Mills, R. T. E., & Emmett, B. A. (2014). Evaluation of Dissolved Organic Carbon as a Soil Quality Indicator in National Monitoring Schemes. *PLoS One*, *9*(3), e90882. https://doi.org/10.1371/journal.pone.0090882

Kalbitz, K., Solinger, S., Park, J. H., Michalzik, B., & Matzner, E. (2000). Controls on the dynamics of dissolved organic matter in soils: A review. *Soil Science*, *165*(4), 277–304. https://doi.org/10.1097/00010694-200004000-00001

Kendall, K. A., Shanley, J. B., & McDonnell, J. J. (1999). A hydrometric and geochemical approach to test the transmissivity feedback hypothesis during snowmelt. *Journal of Hydrology*, *219*(3–4), 188–205. https://doi.org/10.1016/s0022-1694(99)00059-1

Knorr, K. H. (2013). DOC-dynamics in a small headwater catchment as driven by redox fluctuations and hydrological flow paths—Are DOC exports mediated by iron reduction/oxidation cycles? *Biogeosciences*, *10*(2), 891–904. https://doi.org/10.5194/bg-10-891-2013

Köhler, S. J., Lidman, F., & Laudon, H. (2014). Landscape types and pH control organic matter mediated mobilization of Al, Fe, U and La in boreal catchments. *Geochimica et Cosmochimica Acta*, *135*, 190–202. https://doi.org/10.1016/j.gca.2014.03.033

Kong, X. Z., Ghaffar, S., Determann, M., Friese, K., Jomaa, S., Mi, C. X., et al. (2022). Reservoir water quality deterioration due to deforestation emphasizes the indirect effects of global change. *Water Research*, *221*, 118721. https://doi.org/10.1016/j.watres.2022.118721

Kothawala, D. N., Ji, X., Laudon, H., Ågren, A. M., Futter, M. N., Köhler, S. J., & Tranvik, L. J. (2015). The relative influence of land cover, hydrology, and in-stream processing on the composition of dissolved organic matter in boreal streams. *Journal of Geophysical Research-Biogeosciences*, *120*(8), 1491–1505. https://doi.org/10.1002/2015jg002946

Kreutzweiser, D. P., Hazlett, P. W., & Gunn, J. M. (2008). Logging impacts on the biogeochemistry of boreal forest soils and nutrient export to aquatic systems: A review. *Environmental Reviews*, *16*(NA), 157–179. https://doi.org/10.1139/a08-006

Laudon, H., Hasselquist, E. M., Peichl, M., Lindgren, K., Sponseller, R., Lidman, F., et al. (2021). Northern landscapes in transition: Evidence, approach and ways forward using the Krycklan Catchment Study. *Hydrological Processes*, *35*(4), e14170. https://doi.org/10.1002/hyp.14170

Lavonen, E. E., Gonsior, M., Tranvik, L. J., Schmitt-Kopplin, P., & Köhler, S. J. (2013). Selective Chlorination of Natural Organic Matter: Identification of Previously Unknown Disinfection Byproducts. *Environmental Science & Technology*, *47*(5), 2264–2271. https://doi.org/10.1021/es304669p

Leach, J. A., Lidberg, W., Kuglerová, L., Peralta-Tapia, A., Ågren, A., & Laudon, H. (2017). Evaluating topography-based predictions of shallow lateral groundwater discharge zones for a boreal lake-stream system. *Water Resources Research*, *53*(7), 5420–5437. https://doi.org/10.1002/2016wr019804

Ledesma, J. L. J. (2025). Daily values of stream discharge, stream DOC and nitrate concentrations, riparian groundwater tables, and riparian soil water DOC and nitrate concentrations at three catchments (Rappbode—Germany, and Font del Regàs and Fuirosos—Spain) for different periods within 2013 to 2023 [Dataset]. *HydroShare*. https://doi.org/10.4211/hs.2da2df3124ee4585b71e6d409dd88387

Ledesma, J. L. J., Futter, M. N., Blackburn, M., Lidman, F., Grabs, T., Sponseller, R. A., et al. (2018). Towards an Improved Conceptualization of Riparian Zones in Boreal Forest Headwaters. *Ecosystems*, *21*(2), 297–315. https://doi.org/10.1007/s10021-017-0149-5

Ledesma, J. L. J., Grabs, T., Bishop, K. H., Schiff, S. L., & Köhler, S. J. (2015). Potential for long-term transfer of dissolved organic carbon from riparian zones to streams in boreal catchments. *Global Change Biology*, *21*(8), 2963–2979. https://doi.org/10.1111/gcb.12872

Ledesma, J. L. J., Kothawala, D. N., Bastviken, P., Maehder, S., Grabs, T., & Futter, M. N. (2018). Stream Dissolved Organic Matter Composition Reflects the Riparian Zone, Not Upslope Soils in Boreal Forest Headwaters. *Water Resources Research*, *54*(6), 3896–3912. https://doi.org/10.1029/2017wr021793

Ledesma, J. L. J., Lupon, A., & Bernal, S. (2021). Hydrological responses to rainfall events including the extratropical cyclone Gloria in two contrasting Mediterranean headwaters in Spain; the perennial Font del Regàs and the intermittent Fuirosos. *Hydrological Processes*, *35*(12), e14451. https://doi.org/10.1002/hyp.14451

Ledesma, J. L. J., Lupon, A., Martí, E., & Bernal, S. (2022). Hydrology and riparian forests drive carbon and nitrogen supply and DOC: NO_3^- stoichiometry along a headwater Mediterranean stream. *Hydrology and Earth System Sciences*, *26*(15), 4209–4232. https://doi.org/10.5194/hess-26-4209-2022

Ledesma, J. L. J., Ruiz-Pérez, G., Lupon, A., Poblador, S., Futter, M. N., Sabater, F., & Bernal, S. (2021). Future changes in the Dominant Source Layer of riparian lateral water fluxes in a subhumid Mediterranean catchment. *Journal of Hydrology*, *595*, 126014. https://doi.org/10.1016/j.jhydrol.2021.126014

Li, A. G., Bernal, S., Kohler, B., Thomas, S. A., Martí, E., & Packman, A. I. (2021). Residence Time in Hyporheic Bioactive Layers Explains Nitrate Uptake in Streams. *Water Resources Research*, *57*(2), e2020WR027646. https://doi.org/10.1029/2020wr027646

Li, L., Sullivan, P. L., Benettin, P., Cirpka, O. A., Bishop, K., Brantley, S. L., et al. (2020). Toward catchment hydro-biogeochemical theories. *Wiley Interdisciplinary Reviews-Water*, *8*(1), e1495. https://doi.org/10.1002/wat2.1495

Lidman, F., Boily, Å., Laudon, H., & Köhler, S. J. (2017). From soil water to surface water—How the riparian zone controls element transport from a boreal forest to a stream. *Biogeosciences*, *14*(12), 3001–3014. https://doi.org/10.5194/bg-14-3001-2017

Löfgren, S., Aastrup, M., Bringmark, L., Hultberg, H., Lewin-Pihlblad, L., Lundin, L., et al. (2011). Recovery of Soil Water, Groundwater, and Streamwater From Acidification at the Swedish Integrated Monitoring Catchments. *Ambio*, *40*(8), 836–856. https://doi.org/10.1007/s13280-011-0207-8

Luke, S. H., Luckai, N. J., Burke, J. M., & Prepas, E. E. (2007). Riparian areas in the Canadian boreal forest and linkages with water quality in streams. *Environmental Reviews*, *15*(NA), 79–97. https://doi.org/10.1139/a07-001

Lupon, A., Bernal, S., Poblador, S., Martí, E., & Sabater, F. (2016). The influence of riparian evapotranspiration on stream hydrology and nitrogen retention in a subhumid Mediterranean catchment. *Hydrology and Earth System Sciences*, *20*(9), 3831–3842. https://doi.org/10.5194/hess-20-3831-2016

Lupon, A., Denfeld, B. A., Laudon, H., Leach, J., & Sponseller, R. A. (2020). Discrete groundwater inflows influence patterns of nitrogen uptake in a boreal headwater stream. *Freshwater Science*, *39*(2), 228–240. https://doi.org/10.1086/708521

Lupon, A., Gómez-Gener, L., Fork, M. L., Laudon, H., Martí, E., Lidberg, W., & Sponseller, R. A. (2023). Groundwater-stream connections shape the spatial pattern and rates of aquatic metabolism. *Limnology and Oceanography Letters*, *8*(2), 350–358. https://doi.org/10.1002/lol2.10305

Lupon, A., Sabater, F., Miñarro, A., & Bernal, S. (2016). Contribution of pulses of soil nitrogen mineralization and nitrification to soil nitrogen availability in three Mediterranean forests. *European Journal of Soil Science*, *67*(3), 303–313. https://doi.org/10.1111/ejss.12344

Marcé, R., von Schiller, D., Aguilera, R., Martí, E., & Bernal, S. (2018). Contribution of Hydrologic Opportunity and Biogeochemical Reactivity to the Variability of Nutrient Retention in River Networks. *Global Biogeochemical Cycles*, *32*(3), 376–388. https://doi.org/10.1002/2017gb005677

Marchi, L., Borga, M., Preciso, E., & Gaume, E. (2010). Characterisation of selected extreme flash floods in Europe and implications for flood risk management. *Journal of Hydrology*, *394*(1–2), 118–133. https://doi.org/10.1016/j.jhydrol.2010.07.017

McClain, M. E., Boyer, E. W., Dent, C. L., Gergel, S. E., Grimm, N. B., Groffman, P. M., et al. (2003). Biogeochemical hot spots and hot moments at the interface of terrestrial and aquatic ecosystems. *Ecosystems*, *6*(4), 301–312. https://doi.org/10.1007/s10021-003-0161-9

McDowell, W. H., Bowden, W. B., & Asbury, C. E. (1992). Riparian nitrogen dynamics in two geomorphologically distinct tropical rain-forest watersheds: Subsurface solute patterns. *Biogeochemistry*, *18*(2), 53–75. https://doi.org/10.1007/bf00002703

Musolff, A., Fleckenstein, J. H., Opitz, M., Büttner, O., Kumar, R., & Tittel, J. (2018). Spatio-temporal controls of dissolved organic Carbon stream water concentrations. *Journal of Hydrology*, *566*, 205–215. https://doi.org/10.1016/j.jhydrol.2018.09.011

Musolff, A., Selle, B., Büttner, O., Opitz, M., & Tittel, J. (2017). Unexpected release of phosphate and organic carbon to streams linked to declining nitrogen depositions. *Global Change Biology*, *23*(5), 1891–1901. https://doi.org/10.1111/gcb.13498

Musolff, A., Tarasova, L., Rinke, K., & Ledesma, J. L. J. (2024). Forest Dieback Alters Nutrient Pathways in a Temperate Headwater Catchment. *Hydrological Processes*, *38*(10), e15308. https://doi.org/10.1002/hyp.15308

Musolff, A., Zhan, Q., Dupas, R., Minaudo, C., Fleckenstein, J. H., Rode, M., et al. (2021). Spatial and Temporal Variability in Concentration-Discharge Relationships at the Event Scale. *Water Resources Research*, *57*(10), e2020WR029442. https://doi.org/10.1029/2020wr029442

Naiman, R. J., & Décamps, H. (1997). The ecology of interfaces: Riparian zones. *Annual Review of Ecology and Systematics*, *28*(1), 621–658. https://doi.org/10.1146/annurev.ecolsys.28.1.621

Neubauer, E., Köhler, S. J., von der Kammer, F., Laudon, H., & Hofmann, T. (2013). Effect of pH and Stream Order on Iron and Arsenic Speciation in Boreal Catchments. *Environmental Science & Technology*, *47*(13), 7120–7128. https://doi.org/10.1021/es401193j
Nyberg, L. (1995). Water flow path interactions with soil hydraulic properties in till soil at Gårdsjön, Sweden. *Journal of Hydrology*, *170*(1–4), 255–275. https://doi.org/10.1016/0022-1694(94)02667-z
Peñarroya, X., Lupon, A., Triadó-Margarit, X., Martí, E., Ledesma, J. L. J., Ribot, M., et al. (2023). Dissolved organic carbon bioreactivity and DOC: DIN stoichiometry control ammonium uptake in an intermittent Mediterranean stream. *Freshwater Biology*, *16*(9), 1572–1587. https://doi.org/10.1111/fwb.14152
Peralta-Tapia, A., Sponseller, R. A., Ågren, A., Tetzlaff, D., Soulsby, C., & Laudon, H. (2015). Scale-dependent groundwater contributions influence patterns of winter Baseflow stream chemistry in boreal catchments. *Journal of Geophysical Research-Biogeosciences*, *120*(5), 847–858. https://doi.org/10.1002/2014jg002878
Pinay, G., Bernal, S., Abbott, B. W., Lupon, A., Martí, E., Sabater, F., & Krause, S. (2018). Riparian Corridors: A New Conceptual Framework for Assessing Nitrogen Buffering Across Biomes. *Frontiers in Environmental Science*, *6*, 47. https://doi.org/10.3389/fenvs.2018.00047
Rädler, A. T., Groenemeijer, P. H., Faust, E., Sausen, R., & Púčik, T. (2019). Frequency of severe thunderstorms across Europe expected to increase in the 21st century due to rising instability. *Npj Climate and Atmospheric Science*, *2*(1), 30. https://doi.org/10.1038/s41612-019-0083-7
Raeke, J., Lechtenfeld, O. J., Tittel, J., Oosterwoud, M. R., Bornmann, K., & Reemtsma, T. (2017). Linking the mobilization of dissolved organic matter in catchments and its removal in drinking water treatment to its molecular characteristics. *Water Research*, *113*, 149–159. https://doi.org/10.1016/j.watres.2017.01.066
Rakovec, O., Samaniego, L., Hari, V., Markonis, Y., Moravec, V., Thober, S., et al. (2022). The 2018-2020 Multi-Year Drought Sets a New Benchmark in Europe. *Earth's Future*, *10*(3), e2021EF002394. https://doi.org/10.1029/2021ef002394
Ranalli, A. J., & Macalady, D. L. (2010). The importance of the riparian zone and in-stream processes in nitrate attenuation in undisturbed and agricultural watersheds—A review of the scientific literature. *Journal of Hydrology*, *389*(3–4), 406–415. https://doi.org/10.1016/j.jhydrol.2010.05.045
Riedel, T., Zak, D., Biester, H., & Dittmar, T. (2013). Iron traps terrestrially derived dissolved organic matter at redox interfaces. *Proceedings of the National Academy of Sciences of the United States of America*, *110*(25), 10101–10105. https://doi.org/10.1073/pnas.1221487110
Rodhe, A. (1989). On the generation of stream runoff in till soils. *Nordic Hydrology*, *20*(1), 1–8. https://doi.org/10.2166/nh.1989.0001
Roebuck, J. A., Jr., Prestegaard, K., Jr., Gaviria, C., Myers-Pigg, A., & Ziegler, S. E. (2023). Hydrobiogeochemical controls on the delivery of dissolved organic matter to boreal headwater streams. *Water Resources Research*, *59*(10), e2022WR033358. https://doi.org/10.1029/2022WR033358
Romeiro, J. M. N., Eid, T., Antón-Fernández, C., Kangas, A., & Trømborg, E. (2022). Natural disturbances risks in European Boreal and Temperate forests and their links to climate change-A review of modelling approaches. *Forest Ecology and Management*, *509*, 120071. https://doi.org/10.1016/j.foreco.2022.120071
Sanderman, J., Lohse, K. A., Baldock, J. A., & Amundson, R. (2009). Linking soils and streams: Sources and chemistry of dissolved organic matter in a small coastal watershed. *Water Resources Research*, *45*(3), W03418. https://doi.org/10.1029/2008wr006977
Sawicka, K., Monteith, D. T., Vanguelova, E. I., Wade, A. J., & Clark, J. M. (2016). Fine-scale temporal characterization of trends in soil water dissolved organic carbon and potential drivers. *Ecological Indicators*, *68*, 36–51. https://doi.org/10.1016/j.ecolind.2015.12.028
Schwab, M. P., Klaus, J., Pfister, L., & Weiler, M. (2018). Diel fluctuations of viscosity-driven riparian inflow affect streamflow DOC concentration. *Biogeosciences*, *15*(7), 2177–2188. https://doi.org/10.5194/bg-15-2177-2018
Seibert, J., Grabs, T., Kohler, S., Laudon, H., Winterdahl, M., & Bishop, K. (2009). Linking soil- and stream-water chemistry based on a Riparian Flow-Concentration Integration Model. *Hydrology and Earth System Sciences*, *13*(12), 2287–2297. https://doi.org/10.5194/hess-13-2287-2009
Shafer, M. M., Overdier, J. T., Hurley, J. P., Armstrong, D., & Webb, D. (1997). The influence of dissolved organic carbon, suspended particulates, and hydrology on the concentration, partitioning and variability of trace metals in two contrasting Wisconsin watersheds (USA). *Chemical Geology*, *136*(1–2), 71–97. https://doi.org/10.1016/s0009-2541(96)00139-8
Škerlep, M., Nehzati, S., Sponseller, R. A., Persson, P., Laudon, H., & Kritzberg, E. S. (2023). Differential Trends in Iron Concentrations of Boreal Streams Linked to Catchment Characteristics. *Global Biogeochemical Cycles*, *37*(3), e2022GB007484. https://doi.org/10.1029/2022gb007484
Soued, C., del Giorgio, P. A., & Maranger, R. (2016). Nitrous oxide sinks and emissions in boreal aquatic networks in Quebec. *Nature Geoscience*, *9*(2), 116–120. https://doi.org/10.1038/ngeo2611
Spinoni, J., Vogt, J. V., Naumann, G., Barbosa, P., & Dosio, A. (2018). Will drought events become more frequent and severe in Europe? *International Journal of Climatology*, *38*(4), 1718–1736. https://doi.org/10.1002/joc.5291
Sponseller, R. A., Gundale, M. J., Futter, M., Ring, E., Nordin, A., Näsholm, T., & Laudon, H. (2016). Nitrogen dynamics in managed boreal forests: Recent advances and future research directions. *Ambio*, *45*(Suppl 2), 175–187. https://doi.org/10.1007/s13280-015-0755-4
Stewart, B., Shanley, J. B., Kirchner, J. W., Norris, D., Adler, T., Bristol, C., et al. (2022). Streams as Mirrors: Reading Subsurface Water Chemistry From Stream Chemistry. *Water Resources Research*, *58*(1), e2021WR029931. https://doi.org/10.1029/2021wr029931
Swanson, F. J., Gregory, S. V., Sedell, J. R., & Campbell, A. G. (1982). *Land-water interactions: The Riparian zone*. USDA Forest Service. Retrieved from https://books.google.se/books?id=oxvFjgEACAAJ
Tiegs, S. D., Costello, D. M., Isken, M. W., Woodward, G., McIntyre, P. B., Gessner, M. O., et al. (2019). Global patterns and drivers of ecosystem functioning in rivers and riparian zones. *Science Advances*, *5*(1), eaav0486. https://doi.org/10.1126/sciadv.aav0486
Tittel, J., Buttner, O., Friese, K., Lechtenfeld, O. J., Schuth, S., von Tümpling, W., & Musolff, A. (2022). Iron Exports from Catchments are Constrained by Redox Status and Topography. *Global Biogeochemical Cycles*, *36*(1), e2021GB007056. https://doi.org/10.1029/2021gb007056
Tunaley, C., Tetzlaff, D., Lessels, J., & Soulsby, C. (2016). Linking high-frequency DOC dynamics to the age of connected water sources. *Water Resources Research*, *52*(7), 5232–5247. https://doi.org/10.1002/2015wr018419
Vidon, P., Allan, C., Burns, D., Duval, T. P., Gurwick, N., Inamdar, S., et al. (2010). Hot Spots and Hot Moments in Riparian Zones: Potential for Improved Water Quality Management. *Journal of the American Water Resources Association*, *46*(2), 278–298. https://doi.org/10.1111/j.1752-1688.2010.00420.x
Wania, R., Ross, I., & Prentice, I. C. (2009). Integrating peatlands and permafrost into a dynamic global vegetation model: 2. Evaluation and sensitivity of vegetation and carbon cycle processes. *Global Biogeochemical Cycles*, *23*(15), GB3015. https://doi.org/10.1029/2008gb003413
Wen, H., Perdrial, J., Abbott, B. W., Bernal, S., Dupas, R., Godsey, S. E., et al. (2020). Temperature controls production but hydrology regulates export of dissolved organic carbon at the catchment scale. *Hydrology and Earth System Sciences*, *24*(2), 945–966. https://doi.org/10.5194/hess-24-945-2020

Werner, B. J., Lechtenfeld, O. J., Musolff, A., de Rooij, G. H., Yang, J., Gründling, R., et al. (2021). Small-scale topography explains patterns and dynamics of dissolved organic carbon exports from the riparian zone of a temperate, forested catchment. *Hydrology and Earth System Sciences*, *25*(12), 6067–6086. https://doi.org/10.5194/hess-25-6067-2021

Werner, B. J., Musolff, A., Lechtenfeld, O. J., de Rooij, G. H., Oosterwoud, M. R., & Fleckenstein, J. H. (2019). High-frequency measurements explain quantity and quality of dissolved organic carbon mobilization in a headwater catchment. *Biogeosciences*, *16*(22), 4497–4516. https://doi.org/10.5194/bg-16-4497-2019

Winterdahl, M., Erlandsson, M., Futter, M. N., Weyhenmeyer, G. A., & Bishop, K. (2014). Intra-annual variability of organic carbon concentrations in running waters: Drivers along a climatic gradient. *Global Biogeochemical Cycles*, *28*(4), 451–464. https://doi.org/10.1002/2013gb004770

Wohl, E. (2017). The significance of small streams. *Frontiers of Earth Science*, *11*(3), 447–456. https://doi.org/10.1007/s11707-017-0647-y

Zhi, W., & Li, L. (2020). The Shallow and Deep Hypothesis: Subsurface Vertical Chemical Contrasts Shape Nitrate Export Patterns from Different Land Uses. *Environmental Science & Technology*, *54*(19), 11915–11928. https://doi.org/10.1021/acs.est.0c01340

Zimmer, M. A., & McGlynn, B. L. (2018). Lateral, Vertical, and Longitudinal Source Area Connectivity Drive Runoff and Carbon Export Across Watershed Scales. *Water Resources Research*, *54*(3), 1576–1598. https://doi.org/10.1002/2017wr021718

References From the Supporting Information

Beiter, D., Weiler, M., & Blume, T. (2020). Characterising hillslope-stream connectivity with a joint event analysis of stream and groundwater levels. *Hydrology and Earth System Sciences*, *24*(12), 5713–5744. https://doi.org/10.5194/hess-24-5713-2020